Palaeontologia Electronica
http://palaeo-electronica.org

VIRTUAL PALAEONTOLOGY: GAIT RECONSTRUCTION OF EXTINCT VERTEBRATES USING HIGH PERFORMANCE COMPUTING

W.I. Sellers, P.L. Manning, T. Lyson, K. Stevens, and L. Margetts

ABSTRACT

Gait reconstruction of extinct animals requires the integration of palaeontological information obtained from fossils with biological knowledge of the anatomy, physiology and biomechanics of extant animals. Computer simulation provides a methodology for combining multimodal information to produce concrete predictions that can be evaluated and used to assess the likelihood of competing locomotor hypotheses. However, with the advent of much faster supercomputers, such simulations can also explore a wider range of possibilities, allowing the generation of gait hypotheses *de novo*. In this paper we document the use of an 8000 core computer to produce mechanically and physiologically plausible gaits and trackway patterns for a sub-adult dinosaur (*Edmontosaurus annectens*), evaluating a large range of locomotor possibilities in terms of running speed. The anatomical reconstruction presented is capable of running and hopping bipedal gaits; trot, pace and single foot symmetrical quadrupedal gaits; and asymmetrical galloping gaits. Surprisingly hopping is the fastest gait (17 ms^{-1}), followed by quadrupedal galloping (16 ms^{-1}) and bipedal running (14 ms^{-1}). Such a hopping gait is considered unlikely for this animal, which would imply that either our anatomical and physiological reconstruction is incorrect or there are important constraints such as skeletal loading and safety factor that are currently not included in our simulation. The most likely errors are in joint ranges of motion, combined with the lengths of muscle fibres and tendons since these values are difficult to reconstruct. Thus the process of gait simulation is able to narrow down our predictions of unknown features of the extinct animal using a functional bracket. Trackway geometries derived from the gait models are currently very basic due to the simplicity of the ground/foot contact model used, but demonstrate the future potential of this technology for interpreting and predicting trackway geometry.

W.I. Sellers. Lecturer in Integrative Vertebrate Biology, Faculty of Life Sciences, The University of Manchester, Jackson's Mill, PO Box 88, Sackville Street, Manchester M60 1QD, UK, William.Sellers@manchester.ac.uk
P.L. Manning. Senior Lecturer in Palaeontology, School of Earth, Atmospheric and Environmental Sciences, University of Manchester, Manchester, M13 9PL, UK.
T. Lyson. Graduate Student, Department of Geology and Geophysics, Yale University, New Haven, USA.
K. Stevens. Professor of Computer Science, Department of Computer and Information Science, Deschutes Hall, University of Oregon, Eugene, OR 97403.

PE Article Number: 12.3.13A

Submission: 15 November 2008. Acceptance: 2 July 2009

Sellers, W.I., Manning, P.L., Lyson, T., Stevens, K., and Margetts, L., 2009. Virtual Palaeontology: Gait Reconstruction of Extinct Vertebrates Using High Performance Computing. *Palaeontologia Electronica* Vol. 12, Issue 3; 11A: 26p;
http://palaeo-electronica.org/2009_3/180/index.html

L. Margetts . Visiting Lecturer in Geology, School of Earth, Atmospheric and Environmental Sciences, University of Manchester, Manchester, M13 9PL, UK.

Keywords: locomotion; dinosaur; Hadrosaur; robotics; simulation

INTRODUCTION

Computational techniques are now regularly used to investigate the locomotion of extinct species. For example finite element analysis is now frequently used to investigate the strength of skeletal elements under load (Rayfield et al. 2001; Manning et al. 2006; Sereno et al. 2007), and imaging techniques such as LIDAR are powerful tools in the analysis of fossil trackways of vertebrates (Bates et al. 2008). However the most directly applicable technique is locomotor modelling. Models vary from the highly theoretical (e.g., Alexander 1992; McGeer 1992; Minetti and Alexander 1997; Srinivasan and Ruina 2006) to more realistic simulations (e.g., Yamazaki et al. 1996; Sellers et al. 2003; Nagano et al. 2005), and these approaches have been used both to understand the fundamental mechanics of terrestrial gait and also to predict gait parameters: either those internal values that are difficult to measure directly or for fossil vertebrates where experimentation is impossible.

Simple models have the great advantage of being straightforward to understand and unequivocal in their predictions. More complex models depend on a much greater number of modelling parameters and are therefore more difficult to interpret. However, because they are based more closely on real organisms they can be directly tested through comparison of their predictions to those obtained experimentally. For example Srinivasan and Ruina's recent model (Srinivasan and Ruina 2006) predicts that there are three types of stable, efficient bipedal locomotion that they describe as walking, pendular running and running. The model itself is highly simplified with mass-less, linear sprung limbs and a point mass body, and so its predictions cannot be tested experimentally. More realistic models are similarly able to produce these gaits spontaneously (Sellers et al. 2004; Sellers et al. 2005) but because they are more closely modelled on the morphology of experimental subjects, their predictions are more accurate and can be directly compared with experimental data.

The earliest musculoskeletal models for use in reconstructing gait in vertebrate fossils date back to the pioneering work of Yamazaki et al. (Yamazaki et al. 1996) who produced a highly sophisticated neuromusculoskeletal simulation to investigate the evolution of bipedality in humans and other primates. Indeed it is early human fossils that have received the most attention with a number of models of extinct bipeds having been produced (Crompton et al. 1998; Kramer 1999; Sellers et al. 2004; Nagano et al. 2005; Sellers et al. 2005; Ogihara and Yamazaki 2006). However, the study of terrestrial vertebrate locomotion has also involved computer simulations: terror birds (Blanco and Jones 2005) and dinosaurs (Gatesy et al. 1999; Stevens 2002; Hutchinson et al. 2005; Sellers and Manning 2007).

Simulations require a musculoskeletal model and are either kinematically based where a movement pattern is provided for the animal based on either trackway data or motion-capture information from extant species, or kinetically based where the simulation is driven by muscular forces usually with a global optimisation criterion to produce efficient models of high speed locomotion. The latter approach is particularly valuable in situations where there are no suitable modern analogues (usually because a particular morphological form is no longer found) or where there is little trackway data (for example most forms of high speed locomotion). Simulation technology is now relatively mature with a range of both commercial [e.g., SC.ADAMS (www.mscsoftware.com), SDFast (www.sdfast.com), MADYMO (www.tass-safe.com)] and open-source [e.g., Dynamechs (dynamechs.sourceforge.net), ODE (opende.sourceforge.net), PhysSym (phys-sim.sourceforge.net) and Tokamac (www.tokamak-physics.com)] along with front ends that allow simplified construction of biomechanical models [e.g., SIMM (www.musculographics.com), OpenSIMM (www.simmtk.org), Marilou Robotics Studio (www.anykode.com), and LifeMod (www.lifemodeler.com)]. Gait production also requires gait controllers, and for complex models it is impractical to explore exhaustively the whole solution space so a selective search is needed to find suitable controller parameters. Popular techniques are to use finite steps within the search space (Srinivasan and Ruina 2006); to constrain parts of the model using functional linkage and pre-designed neural net-

FIGURE 1. *Edmontosaurus annectens*, composite cast of sub-adult based upon remains from Corson County (South Dakota, USA) in the Hell Creek Formation (BHI 126950).

works (Yamazaki et al. 1996); and to use genetic algorithms to explore selectively profitable areas of the search space (Sellers et al. 2003). These approaches are frequently combined with genetic algorithms and this combined approach is particular popular in robotics leading to the term evolutionary robotics (Nolfi and Floreano 2000).

Hadrosaurian dinosaurs are an ideal study animal for gait reconstruction given they were particularly diverse, and their fossil remains relatively abundant (Horner et al. 2004). Trackway interpretations have suggested that they were gregarious (Carpenter 1992; Lockley and Matsukawa 1999). Their gait is particularly interesting because there has been a debate on the function of their well-developed ossified tendons arrayed along their spinal columns (Organ 2006), and also as to whether they were quadrupedal, bipedal or indeed facultatively able to switch between the two gaits (Galton 1970; Maryańska and Osmólska 1984; Lockley 1992; Meyer and Thuring 2003). Added to that a number of extraordinarily well-preserved specimens have been found with probable soft tissue preservation (for review see Manning 2008). One particular aspect of gait that has received considerable attention is the prediction of maximal running speed. Chasing down prey is a vital factor in the lives of extant predators, as is the avoidance of being captured for prey animals. It is, therefore, of little surprise that speed estimation is of such interest to vertebrate palaeobiologists. Recent work estimating dinosaur maximum running speeds (Sellers and Manning 2007) provided a good match between predicted and simulated top speeds of extant bipeds. However, the results for bipedal dinosaurs were surprising in that there was a strong inverse relationship between body mass and top speed. Theoretical considerations have suggested that maximal running speed should be independent of body mass (Hill 1950) or should increase with body mass (Blanco and Gambini 2007). However, experimental and observational data suggest that there is an optimum body size for running speed at about 100 kg with both smaller and larger animals running slower (Garland 1983). These data suggest that simple theoretical models are unable to adequately represent the diversity of physical processes involved in maximal speed running and in particularly the differences associated with varying gaits (bipedal, quadrupedal, symmetrical and asymmetrical), and it is this aspect that is the focus of this paper.

METHODS

Following on from previous work, we used the GaitSym simulation system based on the Open Dynamics Engine (ODE) (Sellers and Manning 2007). To produce the musculoskeletal model, a mounted skeleton of a juvenile *Edmontosaurus annectens* (BHI 126950) was photographed (Figure 1) and measured, and selected elements were laser scanned using a Polhemus FastSCAN system (complete hindlimb and forelimb, limb girdles, skull and representative vertebrae and ribs). This system allows detailed scanning using a short-range laser scanner with the advantage that both the scanning head and the object being scanned can be freely moved, which is especially useful when scanning complex objects such as vertebrae

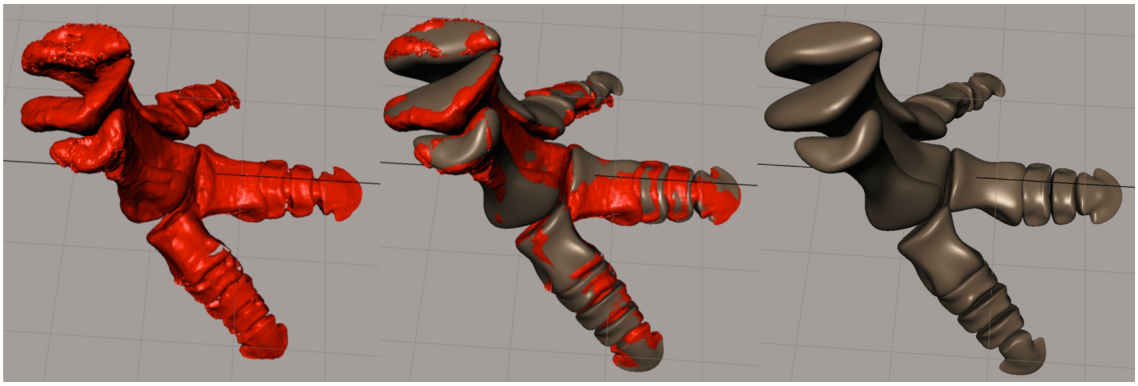

FIGURE 2. Reconstruction of *Edmontosaurus* foot using Maya. Left shows scanned bones with uncorrected taphonomic distortion, Centre shows combined fossil and re-inflated bone, Right shows a re-inflated foot ready to be used in a musculoskeletal model.

and skulls. The raw scan files were exported from the proprietary FastSCAN software in .obj format and imported into Maya (www.autodesk.com) where bone outlines were fitted to the scans (Figure 2). This process allows correcting for distortion, and the idealised geometries produced have a much lower polygon count, which allows them to be used efficiently for later visualisation, animation and modelling. The individual, re-inflated bones are then articulated within Dinomorph (www.dinomorph.com) where joint centres and ranges of motion are defined, and the rearticulated model is re-exported to Maya to allow the construction of the body segment geometry and to define origin and insertion points of muscles (Figure 3) for import into GaitSym. A detailed description of the recommended workflow for creating models can be found in the GaitSym user manual available at www.animalsimulation.org.

With current technology it is relatively easy to simulate the contraction of a large number of muscles, but treating each muscle as a separate entity (or even functionally subdividing muscles) produces extremely complex gait controllers, and our current system cannot find suitable contraction patterns in a reasonable length of time. The complexity can be reduced considerably by grouping functionally equivalent muscles. The hindlimb musculature was taken from Dilkes (2000) and the forelimb musculature from Schachner (2005) and

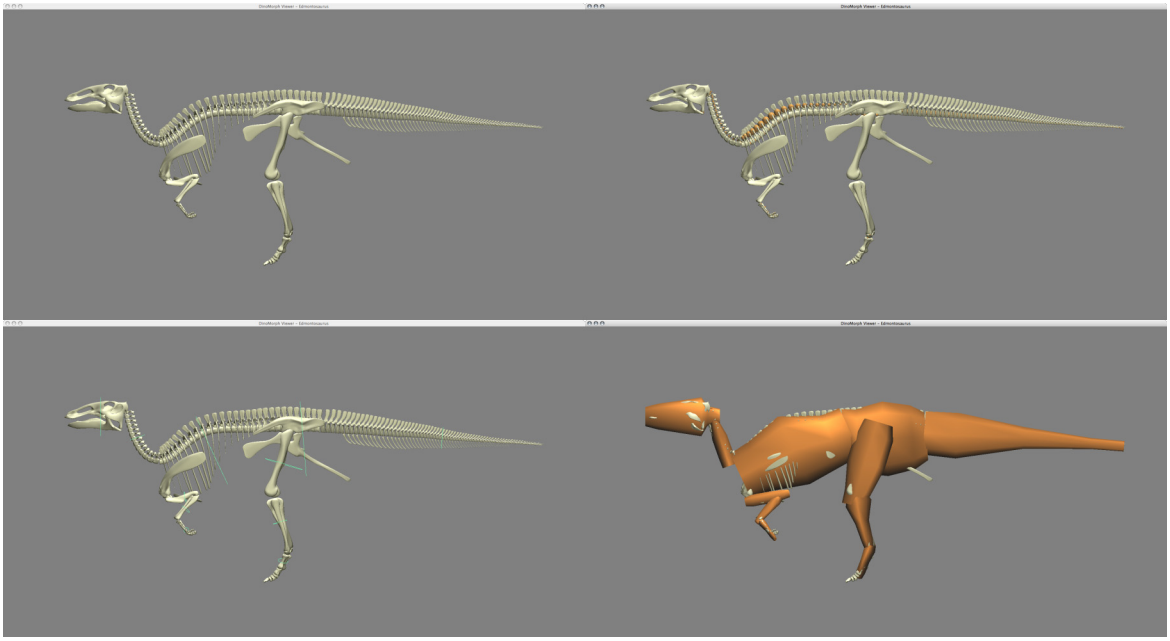

FIGURE 3. Reconstructing the *Edmontosaurus* skeleton. TL rearticulation; TR joint definition; BL defining body hoops; BR lofting estimated body surfaces.

TABLE 1. Per limb muscle proportions for quadrupedal and bipedal models. BM - Body Mass, PCA - Physiological Cross-section Area, FL - Fibre Length, TL - Tendon Length, FD - *Flexor Digitorum*, ED - *Extensor Digitorum*. FL and TL are the same in both quadrupedal and bipedal models.

		Quadruped				Biped	
		% BM (kg)	PCA (m^2)	FL (m)	TL (m)	% BM (kg)	PCA (m^2)
Hindlimb	Deep Dorsal Group	2.33%	0.152	0.104	0.082	3.33%	0.217
	Triceps Femoris Group	1.75%	0.018	0.664	0.201	2.50%	0.026
	Caudo Femoralis Group	3.50%	0.063	0.375	0.496	5.00%	0.090
	Femoro Tibialis Group	1.75%	0.076	0.157	0.470	2.50%	0.108
	Flexor Cruris Group	2.33%	0.030	0.521	0.289	3.33%	0.043
	Gastrocnemius Lateralis + FD	1.75%	0.055	0.215	0.623	2.50%	0.079
	Tibialis Anterior + ED	2.33%	0.191	0.083	0.369	3.33%	0.272
	Gastrocnemius Medialis	1.75%	0.252	0.047	0.649	2.50%	0.359
Forelimb	Shoulder Flexors	1.00%	0.027	0.246	0.267	0%	0
	Triceps Brachii	0.75%	0.030	0.171	0.239	0%	0
	Shoulder Extensors	1.50%	0.162	0.063	0.485	0%	0
	Biceps Brachii	0.50%	0.021	0.160	0.302	0%	0
	Elbow Flexors	0.50%	0.035	0.098	0.016	0%	0
	Elbow Extensors	0.75%	0.108	0.047	0.138	0%	0
	Wrist Flexors	1.00%	0.252	0.027	0.298	0%	0
	Wrist Extensors	1.50%	0.323	0.031	0.353	0%	0

composite muscle groupings produced depending on action (groupings named after Carrano and Hutchinson 2002). Deciding the muscle mass to assign is problematic, but for consistency with previous work we chose a figure of 30% of body mass for extensor musculature (Hutchinson 2004; Hutchinson 2004; Sellers and Manning 2007) and 20% of body mass for flexor muscle mass (Sellers and Manning 2007). However, we note that these values are likely to be towards the upper end of plausible muscle mass estimates (Grand 1977; Hutchinson and Garcia 2002). Dividing this total muscle mass among even a simplified range of muscles is similarly difficult and so the pragmatic solution of dividing equally among the joints of each leg was chosen and in the case of the quadrupedal simulation an arbitrary division was made such that 30% of the muscle mass was in the forelimb and 70% in the hindlimb reflecting the covariation in limb geometry for *Edmontosaurus*. Even then there are muscle groups that have an action over more than one joint, and in these cases they receive a mass proportion from each joint. The fibre lengths and tendon lengths were calculated by measuring the minimum and maximum length of each composite muscle obtained by moving the joints through their full ranges of motion and using the length change for the fibre length and the mean overall length minus the fibre length as the tendon length. This is likely to be a fairly optimal length for any muscle since vertebrate muscles are typically able to generate force from approximately 60% to 160% of their resting length (McGinnis 1999). Using length change through joint range of motion as a way of defining fibre length also eliminates any uncertainty over moment arm since the leverage gain of a larger moment arm is exactly balanced by the force production loss for a given mass of muscle. Physiological cross section area is calculated from fibre length and muscle volume assuming a muscle density of 1056 kg m^{-3} (Winter 1990). All muscle information is shown in Table 1. Segmental mass properties were generated automatically from the body outlines using a body density of 1000 kg m^{-3} (Henderson 1999). The total volume was also used to estimate a total body

mass of 715.3 kg. Limited experimentation was performed using alternative densities and including air sacs (Alexander 1989) but the differences found were small and have therefore been ignored since the uncertainty in the body outlines is likely to be a much larger source of error. The models are fully three-dimensional but all joints are hinge joints allowing only parasagittal rotation to keep the model at manageable levels of complexity. The full specification of each model as a human readable XML file is available for download from http://www.animalsimulation.org. The version for galloping is included in the Appendix.

The muscles were activated by a 5-phase pattern. This was applied to each muscle for a fixed duration, and then the left and right hand side patterns were swapped and reapplied. A complete gait cycle thus consisted of 5 distinct activation patterns for 32 muscles plus the cycle duration: a total of 161 parameters. The musculoskeletal model as placed in a stationary, upright pose with the forelimb tightly flexed in the bipedal models but extended in the quadrupedal model, and this was used as the starting condition for the genetic algorithm optimisation process. This process has been described in detail elsewhere (Sellers et al. 2003; Sellers and Crompton 2004; Sellers et al. 2005) but in brief it proceeds by cycling through a testing phase, a selection phase and a reproduction phase. We start with 1000 random activation patterns, and these patterns are tested by applying these to the model and running the simulation to see how far that activation pattern can drive the model forward in 5 seconds of simulated time. This test evaluates the fitness of these patterns with the fittest being able to drive the model a little further forward than the others. This procedures is then followed by a selection phase where 'roulette wheel' algorithm (Davis 1991) is used to select which of the original 1000 patterns is used as a model, which means that the best of the previous patterns are more likely to contribute to subsequent patterns, and the best 100 patterns are retained for subsequent generations in any case. In this algorithm the roulette wheel is biased so the likelihood of random selection is proportional to the forward distance achieved by the pattern.

In the reproduction phase another 1000 patterns are then created using the selected patterns as models and then adding a small amount of random variation or by merging parts of two patterns (this alteration process is sometimes referred to as mutation). The new patterns are then entered into the cyclic process again where they are tested, selected and reproduced as before. There is a reasonable likelihood that one of the new patterns will work better than the ones in the previous generation. This process is repeated 1000 times or until no improvement has been detected for 100 repeats. At the end of this process, from a standing start, some form of forward locomotion will have been generated. Rather than begin again from a standing start with a new random set of patterns, a new set of initial conditions are generated from the simulation by taking a snapshot of the model state after one gait cycle. This state is now a dynamic starting condition with velocities as well as positions for all the segments and enables us to bootstrap the simulation process since we are aiming to simulate steady state locomotion rather than acceleration. We also use the previous best set of patterns as the starting set of patterns since these are likely to be good patterns for the new starting conditions. The whole process (1000 batches of new patterns) is then repeated, and this process of restarting from a new set of initial conditions generated from a previous run is repeated 20 times. This simulation has potentially been run 20 × 1000 × 1000 times although usually because of the termination after no improvement rule it is usually about half this value i.e., 10,000,000 repeats. In this particular project this process was performed for both the bipedal model and for the quadrupedal model, and each model was repeated 10 times. Given that the simulator runs in roughly half real time, over 10,000 days of CPU time is represented. Fortunately the system is able to run on multiple computers simultaneously so this amount of computing power is relatively manageable.

After optimisation, the best runs are chosen from each of the 20 top level repeats, and these are visualised and the gait classified. The gaits are generated randomly, and the same selective effort has been put into each case so these should be an unbiased estimate of the locomotor capabilities of the quadrupedal and bipedal forms. The random noise added is normally distributed so given long enough each run can theoretically explore the whole of the gait search space. Experience has shown that with this amount of computational effort it will tend to stabilise around a local rather than a global optima that allows it to find a range of sub-optimal gaits but to produce high quality gait within these sub-optima. However, it was hoped that with 10 repeats it would be possible to detect patterns of preferred gait: gaits that either occupy a large proportion of the search space or that produce consistently higher speed than other gaits. The gait

TABLE 2. Descriptions of the gaits generated by the simulator including the top speed attained.

Quadrupeded	V (ms^{-1})	Description
	8.0	Skipping hindlimb with minimal forelimb contribution
	10.4	Trotting gait
	10.5	More of less bipedal with odd skipping gait, minimal forelimb contribution
	10.6	Diagonal single foot gait
	11.4	More or less bipedal run, no regular forelimb contribution
	12.0	More or less bipedal run, no regular forelimb contribution
	12.4	Pacing gait
	12.6	Gallop but without a very organised or consistent forelimb contribution
	13.1	Pacing gait
	13.7	Galloping gait
Biped	6.3	Irregular hop/skip
	7.2	Irregular run
	7.4	Irregular run
	8.4	Run
	9.0	Run
	9.3	Slightly irregular run
	10.8	Slightly irregular run
	11.1	Slightly irregular hop/skip
	11.5	Hop
	16.5	Hop

types produced were visually identified. Selected gaits were also further optimised using a lower total run time (3 seconds) to see whether the requirements of stability were hampering their maximum running speed.

RESULTS

All runs produced effective forward gait but there was a surprisingly large variation in the gaits generated and the maximum speeds. Table 2 summarizes the results.

The quadrupedal model never generated a completely bipedal run but in 3 out of 10 occasions the contribution of the forelimb was minimal: brushing along the ground momentarily at some point in the gait cycle. The other seven gaits generated were quadrupedal, and the full range of symmetrical gaits were demonstrated: trot, pace and single foot (Hildebrand 1965). However, given the essentially symmetrical nature of the muscle pattern generator it was surprising that the highest speed gait discovered was the asymmetrical gallop. The enforced bipedal model generated a range of hopping and primarily running gaits. The surprising finding was that the fastest gait seen was a kangaroo style hop.

Of these gaits, three were identified as interesting and were re-optimised for a 3 second duration rather than a 5 second duration to reduce the effects of stability that seemed to particularly effect the bipedal runs. All top speeds increased (bipedal run 14.0, quadrupedal gallop 15.7, bipedal hop 17.3) but the biggest increase was for the bipedal run. The bipedal run and gallop as well as the quadrupedal gallop can be seen as pre-rendered movies (Movie 1, 2 and 3).

The simulator can also calculate the ground reaction force generated by the model, which can be rendered as a virtual trackway (Figure 4). The foot/substrate contact model is highly simplified being represented as contact spheres attached to the distal ends of the digits. To produce the contact maps, these point forces have been smeared over a larger area to be more representative of a hadro-

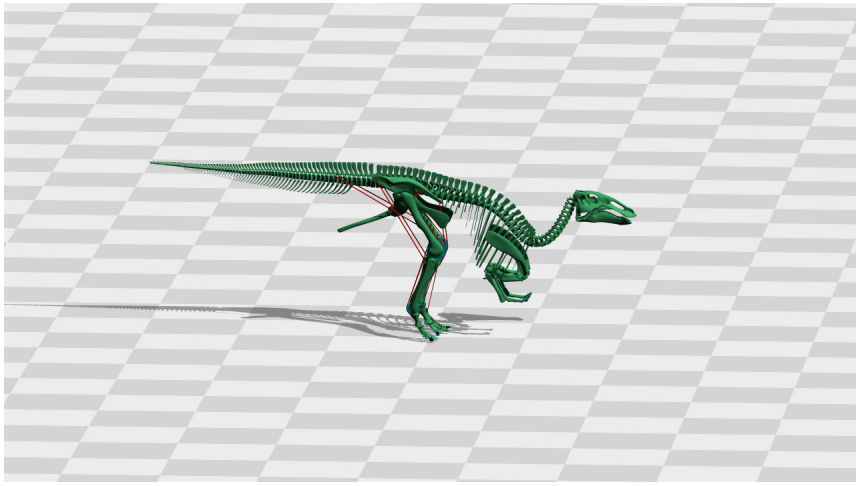

MOVIE 1. Bipedal hopping gait generated by the simulator. Playback is at approximately quarter speed (24 fps from a 100 fps original).

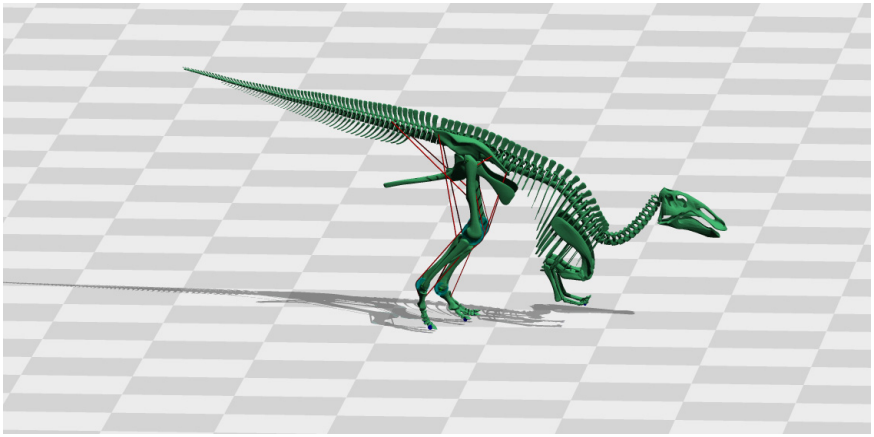

MOVIE 2. Bipedal running gait generated by the simulator. Playback is at approximately quarter speed (24 fps from a 100 fps original).

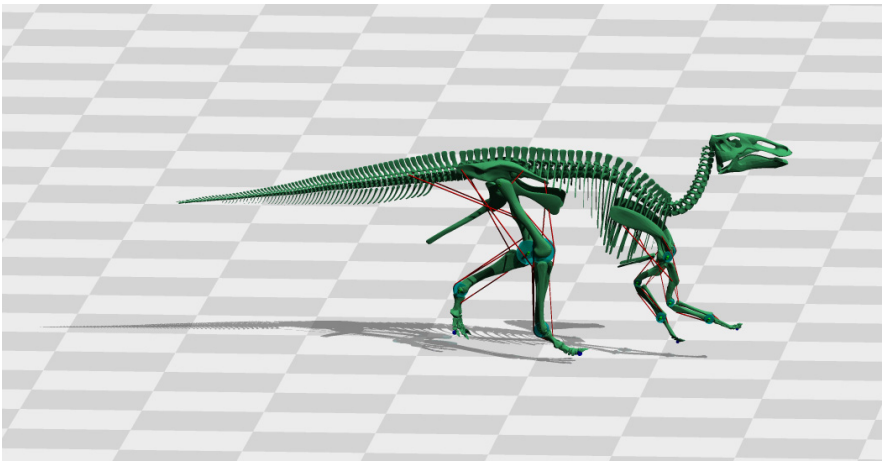

MOVIE 3. Quadrupedal galloping gait generated by the simulator. Playback is at approximately quarter speed (24 fps from a 100 fps original).

TABLE 3. Peak mid-shaft skeletal loading for each of the models. Positive values represent peak compressive stress and negative values peak tensile stress. All values are in MPa.

	Bipedal Hop 16.5 ms^{-1}	Bipedal Run (MPa) 14.0 ms^{-1}	Quadrupedal Gallop 13.7 ms^{-1}
Femur Min	-555	-253	-357
Femur Max	574	269	373
Humerus Min			-710
Humerus Max			716

saur foot. However the differences between the different trackway types can be clearly seen.

DISCUSSION

The simulator has clearly been able to find a large range of gaits that are both physiologically and anatomically possible given the constraints of the model. The fastest gait is the bipedal hop, followed by the quadrupedal gallop and finally the bipedal run. The question then becomes which of these gaits would the animal have chosen? Bipedal hopping would seem to be the obvious answer but this interpretation of the findings would be very bold. It is true that hopping has been described in dinosaurs based on trackway evidence, and an ichniospecies has even been proposed based on a putatively hopping gait: *Saltosauropus latus* (Bernier et al. 1984). However the current interpretation of these ostensibly hopping tracks is that they are swimming traces probably produced by a large turtle (Lockley 2007). The largest hopping mammals are probably the Pleistocene megafaunal species of macropodid *Procoptodon goliah* with a mean estimated body mass of 232 kg (Helgen et al. 2006) so a 715 kg hopper is not an impossibility but identification of hopping based on morphological features is not straightforward. Whilst kangaroos are highly anatomically specialised, other hopping animals are less obvious: *Otolemur garnettii* and *Galago crassicaudatus* are morphologically very similar bushbabies and yet one is a habitual hopper when on the ground whereas the other employs a bounding gallop (Oxnard et al. 1990). However, what is more likely is that the simulation is able to tell us that our reconstruction is incorrect: features of the model that are insufficiently constrained have allowed it to develop a highly effective hopping gait that would not be available for the animal itself.

There are several possibilities here. Firstly hopping may put higher loads on the skeleton than running, and this is not currently incorporated into the simulation. Secondly, ranges of motion on joint, muscle fibre lengths or tendon lengths may allow hopping to occur. Thus the question becomes why could this animal not hop as the simulation shows the current configuration could do so effectively. In the former case the question of skeletal loading during locomotion has received considerable attention. Initial work used beam theory to explain observed differences in skeletal robusticity with body size (McMahon 1973), and this has been used to estimate the athletic ability of dinosaurs (Alexander 1985). More recent work has made considerable use of finite element analysis (FEA) to investigate the detailed loading of individual skeletal elements (Rayfield et al. 2001; Rayfield 2005; Manning et al. 2006; Sereno et al. 2007). Musculoskeletal models allow these numerical analyses to be taken to their next logical step since they calculate the forces in individual muscles and muscle groups as well as the reaction forces and torques around joints. Thus the full in vivo loading environment of skeletal elements is available, and following on from work elsewhere (Smith et al. 2007) we are curretnly developing software to integrate high speed FEA of skeletal loading into the current simulation system.

In the latter case, however, diagnosing hopping would require considerably more experimental work on a wide range of extant hopping animals including the development of hopping simulators that match experimental results. However as a preliminary investigation of the current results, we performed a simple beam mechanic analysis of the loads on the femur and humerus based solely on the joint reaction forces calculated by the model (Alexander 1974). This ignores much of the complexity of the actual shape, loading and movement of the bones but does serve to illustrate potential loading differences associated with each gait that may explain actual gait choice. The bones were modelled as thick-walled cylinders using the measured mean external radius and assuming an internal radius half the external radius as is typical for load-bearing bones in mammals (Garcia and da

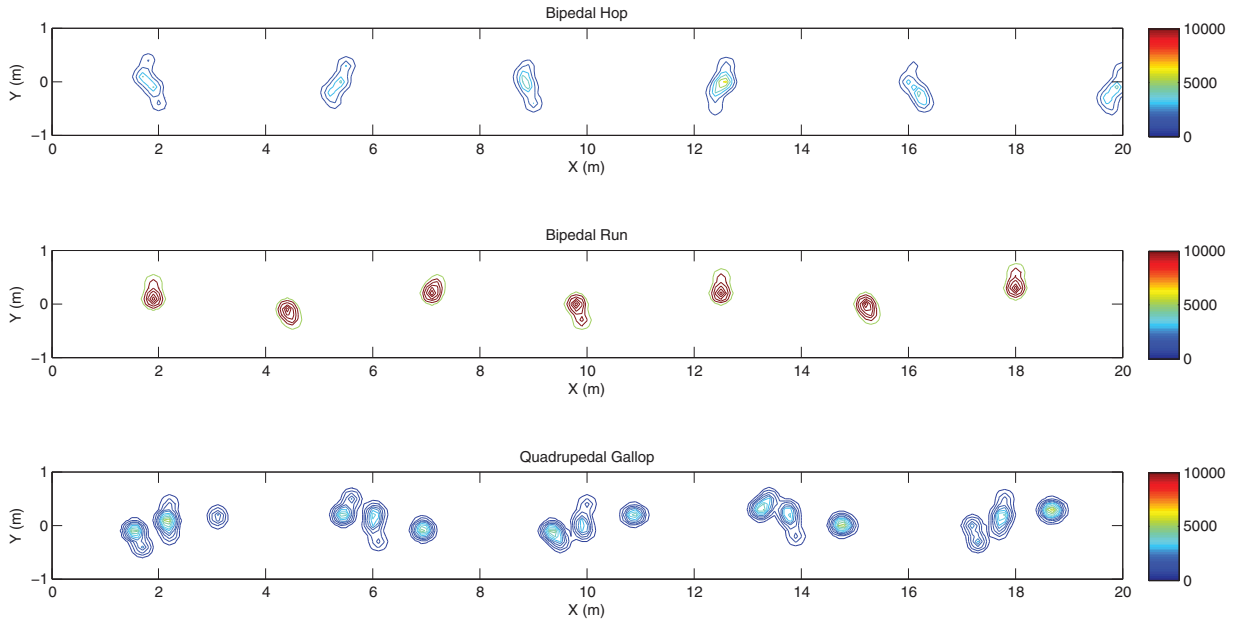

FIGURE 4. Contour plots of the ground reaction forces generated by the model for the three fastest gait types. Top: bipedal hop; middle: bipedal run; bottom quadrupedal gallop.

Silva 2006). In this form of analysis, the bone is assumed to be stationary and fixed at the mid-shaft. Loading is calculated as compressive, and lateral bending components can be combined to estimate the peak tensile and compressive loads. Table 3 shows the results for the three high-speed gait types. It is clear that in this simulation both hopping and galloping generate very high skeletal loads, and the bipedal running results are much lower. The breaking stress of bone is approximately 240 MPa for a 1000 kg animal (Biewener 1982) but it is highly dependent on loading rate, and considerably higher values can be withstood for high strain rates (Reilly and Burstein 1974). However, experimentally measured peak stress values for running animals are much lower than this with typical strain values of 2000 to 3000 microstrain which equates to 40 to 60 MPa (Rubin and Lanyon 1984). This value would suggest that bipedal running is the most likely gait but it must be remembered that the optimisation did not take skeletal loading into account when generating gait. There may be very similar results in terms of top speed that have much lower skeletal loads associated. This area is clearly where research effort needs to be focussed.

The results might be interpreted as weakly supporting bipedal running as the preferred high-speed locomotor mode for *Edmontosaurus*. It is certainly true that recent finds show friction calluses on the manus (Figure 5) but the weight of current thought proposes hadrosaurs to be primarily bipedal with facultative quadrupedalism at low speeds (Galton 1970; Meyer and Thüring 2003). The simulations show that the animal can certainly facultatively switch between bipedalism and quadrupedalism but in fact at high speeds bipedalism was likely to be preferable. However the quadrupedal mode is much more stable than the bipedal one as judged by the much closer range of speed estimates in the 10 independent repeats. The highest speed gallop is faster than the fastest bipedal run even though the amount of locomotor muscle is the same in both cases. Added to that, the quadrupedal gait might be expected to have a better turning speed since it allows force to be applied to the substrate at an increased distance from the centre of mass leading to a greater possible torque (although counter to this argument is the fact that the anterior muscle mass would increase the moment of inertia so that a greater impulse would be required to affect a turn). Turning speed in animals is currently poorly understood.This is an area where there is very little experimental data for comparison. Certainly if an animal has forelimbs that can touch the ground there is very little point in not using them although it is clear that care might be necessary to maintain skeletal loading within acceptable limits. Galloping gaits are unsurprisingly preferred at high speeds, and such gaits are adopted by most high-speed quadrupeds. The idea that an animal might rear-up onto its hind limbs at

FIGURE 5. *Edmontosaurus* sp. manus from MRF-03 showing pad structure (to left) and 3-dimensional (collapsed) skin envelope (Scale bar in cm).

high speed confuses acceleration that might tend to tilt the animal backwards with steady state high-speed running. In terms of medium speed gaits there is overlap between the bipedal and symmetrical gaits with the pace slightly preferred to the trot or single foot. Bipedalism has more appeal at low speed, both because it is supported by trackway evidence (Lockley 1992) and also because that is when the extra mobility in head, neck and cranial trunk may be useful both for predator search behaviour and foraging. The predicted top speeds themselves are entirely reasonable. They are faster than our previous estimates for predatory dinosaurs (Sellers and Manning 2007) but rather slower than modern quadrupeds of equivalent body size. For example, horses are quoted as having running speeds of 70 km/h (19.4 ms^{-1}) (Garland 1983). One could certainly argue that a life-lunch cost-benefit analysis would always assume that a prey animal should invest more in predator avoidance than a prey animal should invest in prey capture.

The virtual trackways should be considered a proof-of-concept rather than being particularly useful. They do show the effects of spacing changes with gait as a function of speed rather well but the current state of ground-substrate interaction simulation within the model is insufficient to provide a good footprint indent. However there is no reason why future versions of the model could not incorporate the improved models currently being developed (Manning 2004; Falkingham et al. In Press). Such simulations would provide a highly effective way of reconstructing the locomotor behaviour of track-makers as well as providing force/time profiles for footprint simulations. It is possible that this technique may allow more accurate estimates of track-maker's speed (Sellers et al. 2005) but the biggest source of uncertainty is always the identity and stature of the track-maker and computer simulation can only help in that area once track simulations have improved.

CONCLUSION

This paper demonstrates what can be achieved with the current level of computer simulation technology. The simulations do demonstrate a wide range of possible locomotor modes and shows (a) that 10 independent repeats is probably insufficient for a quadrupedal gait analysis and (b) that there are major gaps in our understanding of gait choice that are highlighted by this process. Whilst bipedality is currently the most likely option, a high-speed quadrupedal hadrosaur should not be ruled out as a serious locomotor possibility for this group of dinosaurs.

ACKNOWLEDGEMENTS

We would like to thank National Geographic, EPSRC and NERC for their financial support for this project. We also wish to thank the Marmarth

Research Foundation for access to MRF-03 and the Black Hills Institute of Geological Research for access to the cast of the sub-adult *Edmontosaurus*.

REFERENCES

Alexander, R.M. 1974. The mechanics of jumping by a dog (*Canis familiaris*). *Journal of the Zoological Society of London,* 173:549-573.

Alexander, R.M. 1985. Mechanics of posture and gait in some large dinosaurs. *Zoological Journal of the Linnean Society,* 82:1-25.

Alexander, R.M. 1989. *Dynamics of dinosaurs and other extinct giants*. Cambridge University Press; Columbia University Press, Cambridge; New York.

Alexander, R.M. 1992. A model of locomotion on compliant legs. *Philosophical Transactions of the Royal Society B,* 338:189-198.

Bates, K.T., Rarity, F., Manning, P.L., Hodgetts, D., Villa, B., Oms, O., Galobart, À., and Gawthorpe, R.L. 2008. High-resolution LIDAR and photogrammetric survey of the Fumanya dinosaur tracksites (Catalonia): Implications for the conservation and interpretation of geological heritage sites. *Journal of the Geological Society, London,* 165:115-127.

Bernier, P., Barale, G., Bourseau, J.-P., Buffetaut, E., Demathieu, G.R., Gaillard, C., Gall, J.C., and Wenz, S. 1984. Decouverte de pistes de dinosaures sauteurs dans les calcaires lithographiques de Cerin (Kimmeridgian Superieur, Ain, France): implications paleoecologiques. *Géobios, Mémoire Spéciale* 8:177-185.

Biewener, A.A. 1982. Bone strength in small mammals and bipedal birds - do safety factors change with body size. *Journal of Experimental Biology,* 98:289-301.

Blanco, R.E., and Gambini, R. 2007. Maximum running speed limitations on terrestrial mammals: A theoretical approach. *Journal of Biomechanics,* 40:2517-2522.

Blanco, R.E., and Jones, W.W. 2005. Terror birds on the run: a mechanical model to estimate its maximum running speed. *Proceedings of the Royal Society of London B,* 272:1769-1773

Carpenter, K. 1992. Behavior of hadrosaurs as interpreted from footprints in the "Mesaverde" Group (Campanian) of Colorado, Utah, and Wyoming. *Rocky Mountain Geology,* 29:81-96.

Carrano, M.T., and Hutchinson, J.R. 2002. Pelvic and Hindlimb Musculature of *Tyrannosaurus rex* (Dinosauria: Theropoda). *Journal of Morphology,* 253:207-228.

Crompton, R.H., Li, Y., Wang, W., Günther, M.M., and Savage, R. 1998. The mechanical effectiveness of erect and "bent-hip, bent-knee" bipedal walking in *Australopithecus afarensis*. *Journal of Human Evolution,* 35:55-74.

Davis, L. 1991. *Handbook of Genetic Algorithms*. Van Nostrand Reinhold, New York.

Dilkes, D.W. 2000. Appendicular myology of the hadrosaurian dinosaur *Maiasaura peeblesorum* from the Late Cretaceous (Campanian) of Montana. *Transactions of the Royal Society of Edinburgh: Earth Science,* 90:87-125.

Falkingham, P.L., Margetts, L., Smith, I.M., and Manning, P.L. In Press. Reinterpretation of palmate and semipalmate (webbed) fossil tracks: Insights from finite element modelling. *Palaeogeography, Palaeoclimatology, Palaeoecology*.

Galton, P.M. 1970. The Posture of Hadrosaurian Dinosaurs. *Journal of Paleontology,* 44:464-473.

Garcia, G.J.M., and da Silva, J.K.L. 2006. Interspecific allometry of bone dimensions: A review of the theoretical models. *Physics of Life Reviews,* 3:188-209.

Garland, T., Jr. 1983. The relation between maximal running speed and body mass in terrestrial mammals. *Journal of the Zoological Society of London,* 199:157-170.

Gatesy, S.M., Middleton, K.M., Jenkins, F.A., Jr., and Shubin, N.H. 1999. Three-dimensional preservation of foot movements in Triassic theropod dinosaurs. *Nature,* 399(6732):141-144.

Grand, T.I. 1977. Body-weight - its relation to tissue composition, segment distribution, and motor function .1. Interspecific comparisons. *American Journal of Physical Anthropology,* 47:211-240.

Helgen, K.M., Wells, R.T., Kear, B.P., Gerdtz, W.R., and Flannery, T.F. 2006. Ecological and evolutionary significance of sizes of giant extinct kangaroos. *Australian Journal of Zoology,* 54:293-303.

Henderson, D.M. 1999. Estimating the masses and centers of mass of extinct animals by 3-D mathematical slicing. *Paleobiology,* 25:88-106.

Hildebrand, M. 1965. Symmetrical gaits in horses. *Science,* 150:701-708.

Hill, A.V. 1950. The dimensions of animals and their muscular dynamics. *Science Progress,* 38:209-230.

Horner, J.R., Weishampel, D.B., and Forster, C.A. 2004. Hadrosauridae. In Weishampel, D.B., Dodson, P., and Osmólska, H. (eds.), *The Dinosauria*. University of California Press, Berkeley.

Hutchinson, J.R. 2004. Biomechanical modeling and sensitivity analysis of bipedal running ability. I. Extant taxa. *Journal of Morphology,* 262(1):421-440.

Hutchinson, J.R. 2004. Biomechanical modeling and sensitivity analysis of bipedal running ability. II. Extinct Taxa. *Journal of Morphology,* 262:441-461.

Hutchinson, J.R., and Garcia, M. 2002. Tyrannosaurus was not a fast runner. *Nature,* 415:1018-1021.

Hutchinson, J.R., Anderson, F.C., Blemker, S.S., and Delp, S.L. 2005. Analysis of hindlimb muscle moment arms in Tyrannosaurus rex using a three-dimensional musculoskeletal computer model: implications for stance, gait, and speed. *Paleobiology,* 31:676-701.

Kramer, P.A. 1999. Modelling the locomotor energetics of extinct hominids. *Journal of Experimental Biology,* 202:2807-2818.

Lockley, M.G. 1992. A Quadrupedal Ornithopod Trackway from the Lower Cretaceous of La Rioja (Spain): Inferences on Gait and Hand Structure. *Journal of Vertebrate Paleontology,* 12:150-157.

Lockley, M.G. 2007. A tale of two ichnologies: the different goals and potentials of invertebrate and vertebrate (Tetrapod) ichnotaxonomy and how they relate to ichnofacies analysis. *Ichnos,* 14:39-57.

Lockley, M.G., and Matsukawa, M. 1999. Some observations on trackway evidence for gregarious behavior among small bipedal dinosaurs. *Palaeogeography, Palaeoclimatology, Palaeoecology,* 150:25-31.

Manning, P.L. 2004. A new approach to the analysis and interpretation of tracks: examples from the dinosauria, p. 93-123. In McIlroy, D. (ed.), *The Application of Ichnology to Palaeoenvironmental and stratigraphic analysis*. Geological Society, London, Special Publications, London.

Manning, P.L. 2008. *Grave Secrets of Dinosaurs: Soft tissue and hard science*. National Geographic books, Washington D.C.

Manning, P.L., Payne, D., Pennicott, J., and Barrett, P. 2006. Dinosaur killer claws or climbing crampons? *Biology Letters,* 2:110-112.

Maryańska, T., and Osmólska, H. 1984. Postcranial anatomy of Saurolophus angustirostris with comments on other hadrosaurs. *Palaeontologica Polonica,* 46:119-141.

McGeer, T. 1992. Principles of walking and running, p. 114-140. In Alexander, R.M. (ed.), *Advances in Comparative and Environmental Physiology 11. Mechanics of Animal Locomotion*. Springer-Verlag, Berlin.

McGinnis, P.M. 1999. *Biomechanics of Sport and Exercise*. Human Kinetics, Champagne, Illinois.

McMahon, T.A. 1973. Size and shape in biology. *Science,* 179:1201-1204.

Meyer, C.A., and Thüring, B. 2003. The First Iguanodontid Dinosaur Tracks from the Swiss Alps (Schrattenkalk Formation, Aptian). *Ichnos,* 10:221-228.

Minetti, A.E., and Alexander, R.M. 1997. A theory of metabolic costs for bipedal gaits. *Journal of Theoretical Biology,* 186(4):467-476.

Nagano, A., Umberger, B.R., Marzke, M.W., and Gerritsen, K.G.M. 2005. Neuromusculoskeletal computer modeling and simulation of upright, straight-legged, bipedal locomotion of Australopithecus afarensis (A.L. 288-1). *American Journal of Physical Anthropology,* 126:2-13.

Nolfi, S., and Floreano, D. 2000. *Evolutionary Robotics*. MIT Press, Cambridge, Mass.

Ogihara, N., and Yamazaki, N. 2006. Computer Simulation of Bipedal Locomotion: Toward Elucidating Correlations among Musculoskeletal Morphology, Energetics, and the Origin of Bipedalism, p. 167-174. In Ishida, H., Tuttle, R., Pickford, M., and Nakatsukasa, M. (eds.), *Human Origins and Environmental Backgrounds*. Springer, New York.

Organ, C.L. 2006. Biomechanics of ossified tendons in ornithopod dinosaurs *Paleobiology,* 32:652-665.

Oxnard, C.E., Crompton, R.H., and Lieberman, S.S. 1990. *Animal Lifestyles and Anatomies: The Case of the Prosimian Primate*. University of Washington Press, Seattle.

Rayfield, E.J. 2005. Using finite-element analysis to investigate suture morphology: A case study using large carnivorous dinosaurs. *The Anatomical Record Part A: Discoveries in Molecular, Cellular, and Evolutionary Biology,* 283A(2):349-365.

Rayfield, E.J., Norman, D.B., Horner, C.C., Horner, J.R., Smith, P.M., Thomason, J.J., and Upchurch, P. 2001. Cranial design and function in a large theropod dinosaur. *Nature,* 409:1033-1037.

Reilly, D.T., and Burstein, A.H. 1974. The mechanical properties of cortical bone. *The Journal of bone and joint surgery,* 56:1001-1022.

Rubin, C.T., and Lanyon, L.E. 1984. Dynamic strain similarity in vertebrates; an alternative to allometric limb bone scaling. *Journal of Theoretical Biology,* 107:321-327.

Schachner, E.R. 2005. *Pectoral and Forelimb Musculature of the Basal Iguanodontid Tenontosaurus tilletti (Dinosauria- Ornithischia), MSC Thesis, University of Bristol*, Bristol.

Sellers, W.I., and Crompton, R.H. 2004. Using sensitivity analysis to validate the predictions of a biomechanical model of bite forces. *Annals of Anatomy,* 186:89-95.

Sellers, W.I., and Manning, P.L. 2007. Estimating dinosaur maximum running speeds using evolutionary robotics. *Proceedings of the Royal Society of London B,* 274:2711-2716.

Sellers, W.I., Dennis, L.A., and Crompton, R.H. 2003. Predicting the metabolic energy costs of bipedalism using evolutionary robotics. *Journal of Experimental Biology,* 206:1127-1136.

Sellers, W.I., Cain, G.M., Wang, W., and Crompton, R.H. 2005. Stride lengths, speed and energy costs in walking of Australopithecus afarensis: using evolutionary robotics to predict locomotion of early human ancestors. *Journal of the Royal Society Interface,* 5(2):431-441.

Sellers, W.I., Dennis, L.A., Wang, W., and Crompton, R.H. 2004. Evaluating alternative gait strategies using evolutionary robotics. *Journal of Anatomy,* 204:343-351.

Sereno, P.C., Wilson, J.A., Witmer, L.M., Whitlock, J.A., Maga, A., Ide, O., and Rowe, T.A. 2007. Structural Extremes in a Cretaceous Dinosaur. *PLoS ONE,* 2(11):e1230.

Smith, I.M., Margetts, L., Beer, G., and Duenser, C. 2007. Parallelising the boundary element method using ParaFEM, *Proceedings of the Tenth International Conference on Numerical Methods in Geomechanics, NUMOG X*, Rhodes.

Srinivasan, M., and Ruina, A. 2006. Computer optimization of a minimal biped model discovers walking and running. *Nature,* 439:72-75.

Stevens, K.A. 2002. DinoMorph: Parametric Modeling of Skeletal Structures. *Senckenbergiana Lethaea,* 82:23-34.

Winter, D.A. 1990. *Biomechanics and motor control of human movement*. John Wiley and Sons, New York.

Yamazaki, N., Hase, K., Ogihara, N., and Hayamizu, N. 1996. Biomechanical analysis of the development of human bipedal walking by a neuro-musculo-skeletal model. *Folia Primatologia,* 66:253-271.

Appendix

Complete specification of the hadrosaur model. This version includes the driver values required to generate galloping.

```
<?xml version="1.0"?>
<GAITSYMODE>
  <STATE SimulationTime="0"/>
  <IOCONTROL OldStyleInputs="false"/>
  <GLOBAL IntegrationStepSize="1e-4"
GravityVector="0.0 0.0 -9.81" ERP="0.2"
CFM="1e-10" ContactMaxCorrectingVel="100"
ContactSurfaceLayer="0.001"
AllowInternalCollisions="false" BMR="0"
TimeLimit="5" MetabolicEnergyLimit="0"
MechanicalEnergyLimit="0"
FitnessType="DistanceTravelled"
DistanceTravelledBodyID="HT"/>
  <INTERFACE TrackBodyID="HT"
EnvironmentAxisSize="1 1 1"
EnvironmentColour="0.5 0.5 1.0 1.0"
BodyAxisSize="0.1 0.1 0.1" BodyColour=".275
.725 .451 .9" JointAxisSize="0.1 0.1 0.1"
JointColour="0 1 0 1" GeomColour="0 0 1 0.5"
StrapColour="1 0 0 1" StrapRadius="0.005"
StrapForceColour="1 0 0 0.5"
StrapForceRadius="0.01"
StrapForceScale="0.000001"
StrapCylinderColour="0 1 1 0.5"
StrapCylinderLength="0.1"
DrawingOrder="Environment Joint Muscle Geom
Body"/>
  <ENVIRONMENT Plane="0 0 1 0"/>
  <BODY ID="HT" GraphicFile="ht_hull.obj"
Scale="1" PositionLowBound="-10 -1 0.0"
PositionHighBound="1000 1 10"
Offset="0.071370853363158349 -
9.4219898522232949e-05 -1.4276420322582368"
Mass="571.91967814278394"
MOI="35.467054948732468 443.45901409449215
420.93678159649011 -0.46274408883735624
50.392194389226113 0.015575301414043233"
Density="-1" Position="World 0 0
1.3716550848989824" Quaternion="World
0.99770454359839089 -0.0043580001230305752 -
0.067532375554171992 -0.0024555590126144737"
LinearVelocity="12.401420201193885
0.048234022799837663 0.10113881627253112"
AngularVelocity="-0.29817868392487623
0.74649964861457019 0.12217124622782705"/>
  <BODY ID="LeftThigh"
GraphicFile="left_thigh_hull.obj" Scale="1"
PositionLowBound="-10 -1 0.0"
PositionHighBound="1000 1 10"
Offset="0.44524259230361951 -
0.24267163006437489 -1.272116959478172"
Mass="42.37400036566666"
MOI="2.5494657883395786 2.886681458017534
0.52041527044607561 0.038217851162187462
0.4548132296108659 0.086986222471630556"
Density="-1" Position="World -
0.37944703501216193 0.24289876746329406
1.1596809720856798" Quaternion="World
0.99986327261642338 -0.0042251998040302337 -
0.015761032859227461 -0.0026783581916058796"
LinearVelocity="15.101513650062664 -
0.074312204189691131 0.66081062823457881"
AngularVelocity="-0.35033975328662725 -
8.7455374217370725 0.20143992993130427"/>
  <BODY ID="LeftShank"
GraphicFile="left_shank_hull.obj" Scale="1"
PositionLowBound="-10 -1 0.0"
PositionHighBound="1000 1 10"
Offset="0.44784536956295701 -
0.25423894995604207 -0.66910018074046107"
Mass="15.081917241166668"
MOI="0.40764307257214594 0.44731405191911799
0.10632384970216729 -0.00092403911851659582 -
0.11183436002002527 -0.0020490408577721669"
Density="-1" Position="World -
0.52622752335635958 0.25147080094670915
0.70525449985165201" Quaternion="World
0.92939438744127789 -0.0028742484102449212
0.36905426185928236 -0.0040942755437635772"
LinearVelocity="18.620440188079865 -
0.25255160703693524 0.33871368111170563"
AngularVelocity="-0.32994527847390576 -
5.0344330009691989 0.17044241076909039"/>
  <BODY ID="LeftFoot"
GraphicFile="left_foot_hull.obj" Scale="1"
PositionLowBound="-10 -1 0.0"
PositionHighBound="1000 1 10"
Offset="0.52824217186034217 -
0.24345652133462703 -0.2240724416016866"
Mass="6.3933479319999984"
MOI="0.084445760114794419 0.073878881997155407
0.030202243625299819 0.00025059024321312826
0.018202696755688058 -0.0084908119161335813"
Density="-1" Position="World -
0.87176488592125878 0.24030293245971721
0.43249829554078117" Quaternion="World
0.95579207042555125 -0.0031906748516766469
0.29400083797348059 -0.0038529179228283432"
LinearVelocity="20.268774352243 -
0.40326729794103922 -1.4378887468610126"
AngularVelocity="-0.34280777481409103 -
7.375260285790926 0.18999672261409037"/>
  <BODY ID="RightThigh"
GraphicFile="right_thigh_hull.obj" Scale="1"
PositionLowBound="-10 -1 0.0"
PositionHighBound="1000 1 10"
Offset="0.44524212936624091 0.24267148598192351
-1.2721175597186958" Mass="42.37395754700001"
MOI="2.5494597643557939 2.8866708375447456
0.52041099469890195 -0.038217910113828357
0.45480205383710109 -0.086988165315726326"
Density="-1" Position="World -
0.27650685048111701 -0.24272401444901404
1.1966569471328932" Quaternion="World
```

```
0.98060023557473763 -0.0046389024823999328 -
0.19595447424316556 -0.0018715230729268615"
LinearVelocity="12.133491965222774 -
0.037543534858323804 0.29223810443447162"
AngularVelocity="-0.29479753052919266
1.3617851706492758 0.11703303143883377"/>
  <BODY ID="RightShank"
GraphicFile="right_shank_hull.obj" Scale="1"
PositionLowBound="-10 -1 0.0"
PositionHighBound="1000 1 10"
Offset="0.44777574374667545 0.25422629178699513
-0.66905948226573841" Mass="15.079339094500002"
MOI="0.40761068903493353 0.44720317310237018
0.10623657993005366 0.00093238783241814886 -
0.11173839591398642 0.0020454794347930056"
Density="-1" Position="World -
0.11556561659192344 -0.25976959018170165
0.64595041611014459" Quaternion="World
0.99699220177418169 -0.0043824463458763526 -
0.077340286227521801 -0.0024132740706307972"
LinearVelocity="17.114848290849579 -
0.22333009487919347 -1.2125374552796784"
AngularVelocity="-0.40700591501061589 -
19.056943726963055 0.28755065188806656"/>
  <BODY ID="RightFoot"
GraphicFile="right_foot_hull.obj" Scale="1"
PositionLowBound="-10 -1 0.0"
PositionHighBound="1000 1 10"
Offset="0.52807215606083047 0.24342356711426938
-0.22404605213970355" Mass="6.3937735455000002"
MOI="0.084436566792715259 0.073882384716655508
0.030218118654412436 -0.00025860630405514698
0.018223197958682134 0.008497342835060831"
Density="-1" Position="World -
0.11032537506902784 -0.25266772628711776
0.2069874121425879" Quaternion="World
0.98640396777132666 -0.0045768092906801382 -
0.16426253991279316 -0.0020206838195725866"
LinearVelocity="25.568918884634968 -
0.40035947380895737 -1.0338858661525421"
AngularVelocity="-0.41293641523648095 -
20.135813787158515 0.29656099013655796"/>
  <BODY ID="LeftArm"
GraphicFile="left_arm_hull.obj" Scale="1"
PositionLowBound="-10 -1 0.0"
PositionHighBound="1000 1 10" Offset="-
0.69268956944496685 -0.16658494440840449 -
0.61592609661063658" Mass="4.7362533456666664"
MOI="0.049907087247126614 0.079018136000938294
0.037057097114955792 -0.0012936705694527705 -
0.034999355420406608 -0.0015754134243998327"
Density="-1" Position="World
0.81029145325124485 0.15649628762924522
0.70751549903207112" Quaternion="World
0.99702574922530895 -0.0039587763617395227
0.07690665460707706 -0.0030577685616784921"
LinearVelocity="12.108183324816498 -
0.053693948600552481 -0.75228944947689003"
AngularVelocity="-0.30507012850762633 -
0.5075780489067464 0.1326439147689796"/>
  <BODY ID="LeftForearm"
GraphicFile="left_forearm_hull.obj" Scale="1"
PositionLowBound="-10 -1 0.0"
PositionHighBound="1000 1 10" Offset="-
0.67308134034437705 -0.16331368160306101 -
0.34308849378137507" Mass="2.0512079895000004"
MOI="0.015799437534319779 0.023132047750820964
0.008943951190149518 0.00026505662375837064
0.0098226641772959523 -0.00039948382355820726"
Density="-1" Position="World
0.78399253744623731 0.15126500751259012
0.45596631975444946" Quaternion="World
0.99973028766020267 -0.0042434314601332325 -
0.022678829301267803 -0.002648759297455072"
LinearVelocity="12.279446120262486 -
0.13396200804890637 -0.74030444566545339"
AngularVelocity="-0.30648053007596443 -
0.76405387885816711 0.13478303712738424"/>
  <BODY ID="LeftHand"
GraphicFile="left_hand_hull.obj" Scale="1"
PositionLowBound="-10 -1 0.0"
PositionHighBound="1000 1 10" Offset="-
0.83508426926748747 -0.13907729605806479 -
0.082641601601437964" Mass="1.03309238"
MOI="0.0052284097176611482
0.0059675982228598557 0.0018759007731578182
0.00030556638302727424 0.0021898187004173834 -
0.00061144454414326836" Density="-1"
Position="World 0.95750867503413684
0.12396182450171173 0.20333303615788711"
Quaternion="World 0.99973028835854072 -
0.0042433328634663816 -0.022678829140629853 -
0.0026486550490781914"
LinearVelocity="12.476158375805969 -
0.18800614395165091 -0.59937153348884653"
AngularVelocity="-0.30648052973949563 -
0.76405387893108745 0.13478303733462732"/>
  <BODY ID="RightArm"
GraphicFile="right_arm_hull.obj" Scale="1"
PositionLowBound="-10 -1 0.0"
PositionHighBound="1000 1 10" Offset="-
0.69281136793356946 0.16564324440002809 -
0.61600853358313512" Mass="4.7361686123333371"
MOI="0.049911250361925487 0.079032126492164678
0.037056200702229154 0.0012548178747346171 -
0.035004978265535065 0.0015267219736502147"
Density="-1" Position="World
0.97717447294669757 -0.17716058823408382
0.64823464203981518" Quaternion="World
0.95278253671555091 -0.0048183440671644871 -
0.30361227162681348 -0.0013452910228591167"
LinearVelocity="15.202922808338712 -
0.065447049251488476 -0.46890207487642144"
AngularVelocity="-0.37455743828203869 -
13.155437578272981 0.23831278661193001"/>
  <BODY ID="RightForearm"
GraphicFile="right_forearm_hull.obj" Scale="1"
PositionLowBound="-10 -1 0.0"
PositionHighBound="1000 1 10" Offset="-
0.67317816135674458 0.16248996401868518 -
0.34317225300432985" Mass="2.0516586884999994"
MOI="0.015812845847471755 0.023148464008991565
0.0089489996579531581 -0.0002651638051287213
0.0098302552302545424 0.00039937768908864847"
Density="-1" Position="World 1.1080156569819755
-0.17683331645915912 0.39625102157648717"
```

```
Quaternion="World 0.9681273686119497 -
0.0047363509108884578 -0.25040841443568651 -
0.0016096907642349947"
LinearVelocity="20.017255376366556 -
0.11925160827090889 3.4086580362796237"
AngularVelocity="-0.45038335112683603 -
26.899094064959876 0.35234760166500001"/>
  <BODY ID="RightHand"
GraphicFile="right_hand_hull.obj" Scale="1"
PositionLowBound="-10 -1 0.0"
PositionHighBound="1000 1 10" Offset="-
0.83516730502368886 0.13829638131619049 -
0.082724261365819118" Mass="1.0324114568333342"
MOI="0.0052250846912375876
0.0059640730504343245 0.0018736868948854761 -
0.00030470483856247303 0.0021883554246982448
0.00061035415222671216" Density="-1"
Position="World 1.3767149851085376 -
0.15536162791074951 0.24713815570089961"
Quaternion="World 0.96762629135170053 -
0.0047401774720662289 -0.25233772320758308 -
0.0016013896778810134"
LinearVelocity="20.596206988068786 -
0.11523919786259472 5.4825301496962018"
AngularVelocity="-0.22471623764284532
13.997842227855708 0.013743759339826189"/>
  <JOINT ID="RightHip" Type="Hinge"
Body1ID="HT" Body2ID="RightThigh"
ParamLoStop="-0.785398163"
ParamHiStop="0.785398163" HingeAnchor="HT -
0.40112914663684152 -0.15409421989852226
0.14970796774176209" HingeAxis="HT 0 1 0"
StartAngleReference="0.25929708128534829"/>
  <JOINT ID="RightKnee" Type="Hinge"
Body1ID="RightThigh" Body2ID="RightShank"
ParamLoStop="-1.570796327" ParamHiStop="0"
HingeAnchor="RightThigh 0.10294212936624075
0.023271485981923495 -0.33551755971869557"
HingeAxis="RightThigh 0 1 0"
StartAngleReference="-0.2396292693189323"/>
  <JOINT ID="RightAnkle" Type="Hinge"
Body1ID="RightShank" Body2ID="RightFoot"
ParamLoStop="0" ParamHiStop="0.785398163"
HingeAnchor="RightShank -0.13192425625332455
0.025976291786995065 -0.33865948226573817"
HingeAxis="RightShank 0 1 0"
StartAngleReference="0.17518773217656869"/>
  <JOINT ID="LeftHip" Type="Hinge" Body1ID="HT"
Body2ID="LeftThigh" ParamLoStop="-0.785398163"
ParamHiStop="0.785398163" HingeAnchor="HT -
0.40112914663684152 0.15390578010147773
0.14970796774176209" HingeAxis="HT 0 1 0"
StartAngleReference="-0.10364555550966217"/>
  <JOINT ID="LeftKnee" Type="Hinge"
Body1ID="LeftThigh" Body2ID="LeftShank"
ParamLoStop="-1.570796327" ParamHiStop="0"
HingeAnchor="LeftThigh 0.10294212936624036 -
0.023271485981922996 -0.33551755971869579"
HingeAxis="LeftThigh 0 1 0"
StartAngleReference="-0.78751619016521479"/>
  <JOINT ID="LeftAnkle" Type="Hinge"
Body1ID="LeftShank" Body2ID="LeftFoot"
ParamLoStop="0" ParamHiStop="0.785398163"
HingeAnchor="LeftShank -0.13192425625332443 -
0.025976291786995287 -0.33865948226573772"
HingeAxis="LeftShank 0 1 0"
StartAngleReference="0.1591647497700302"/>
  <JOINT ID="RightShoulder" Type="Hinge"
Body1ID="HT" Body2ID="RightArm" ParamLoStop="-
0.785398163" ParamHiStop="0.785398163"
HingeAnchor="HT 0.8960208533631584 -
0.15009421989852226 -0.61239203225823791"
HingeAxis="HT 0 1 0"
StartAngleReference="0.48180187316424339"/>
  <JOINT ID="RightElbow" Type="Hinge"
Body1ID="RightArm" Body2ID="RightForearm"
ParamLoStop="-0.785398163"
ParamHiStop="0.785398163" HingeAnchor="RightArm
-0.10451136793356963 0.0056432444000281967 -
0.10160853358313515" HingeAxis="RightArm 0 1 0"
StartAngleReference="-0.11076054718322098"/>
  <JOINT ID="RightWrist" Type="Hinge"
Body1ID="RightForearm" Body2ID="RightHand"
ParamLoStop="-0.785398163" ParamHiStop="0"
HingeAnchor="RightForearm 0.090571838643254909
0.017389964018685283 -0.12742225300432991"
HingeAxis="RightForearm 0 1 0"
StartAngleReference="0.0039866748198729152"/>
  <JOINT ID="LeftShoulder" Type="Hinge"
Body1ID="HT" Body2ID="LeftArm" ParamLoStop="-
0.785398163" ParamHiStop="0.785398163"
HingeAnchor="HT 0.8960208533631584
0.14990578010147773 -0.61239203225823791"
HingeAxis="HT 0 1 0" StartAngleReference="-
0.28913658838891287"/>
  <JOINT ID="LeftElbow" Type="Hinge"
Body1ID="LeftArm" Body2ID="LeftForearm"
ParamLoStop="-0.785398163"
ParamHiStop="0.785398163" HingeAnchor="LeftArm
-0.10451136793356919 -0.0056432444000283633 -
0.10160853358313438" HingeAxis="LeftArm 0 1 0"
StartAngleReference="0.19932938422182639"/>
  <JOINT ID="LeftWrist" Type="Hinge"
Body1ID="LeftForearm" Body2ID="LeftHand"
ParamLoStop="-0.785398163" ParamHiStop="0"
HingeAnchor="LeftForearm 0.090571838643260016 -
0.01738996401868359 -0.1274222530043268"
HingeAxis="LeftForearm 0 1 0"
StartAngleReference="1.1990408665951691e-11"/>
  <GEOM ID="RightFootPP1Contact" Type="Sphere"
BodyID="RightFoot" Radius="0.018"
SpringConstant="2e6" ContactSoftERP="0.1"
Mu="1.0" Abort="false" Position="RightFoot
0.090072156060830466 0.14402356711426945 -
0.20604605213970359" Quaternion="RightFoot 1 0
0 0"/>
  <GEOM ID="RightFootPP2Contact" Type="Sphere"
BodyID="RightFoot" Radius="0.00179"
SpringConstant="2e6" ContactSoftERP="0.1"
Mu="1.0" Abort="false" Position="RightFoot
0.16527215606083046 0.00822356711426947 -
0.20614605213970358" Quaternion="RightFoot 1 0
0 0"/>
  <GEOM ID="RightFootPP3Contact" Type="Sphere"
BodyID="RightFoot" Radius="0.0219"
SpringConstant="2e6" ContactSoftERP="0.1"
```

```
Mu="1.0" Abort="false" Position="RightFoot
0.15507215606083047 -0.11787643288573055 -
0.20214605213970357" Quaternion="RightFoot 1 0
0 0"/>
  <GEOM ID="LeftFootPP1Contact" Type="Sphere"
BodyID="LeftFoot" Radius="0.018"
SpringConstant="2e6" ContactSoftERP="0.1"
Mu="1.0" Abort="false" Position="LeftFoot
0.090072156060830022 -0.14402356711426878 -
0.20604605213970353" Quaternion="LeftFoot 1 0 0
0"/>
  <GEOM ID="LeftFootPP2Contact" Type="Sphere"
BodyID="LeftFoot" Radius="0.00179"
SpringConstant="2e6" ContactSoftERP="0.1"
Mu="1.0" Abort="false" Position="LeftFoot
0.16527215606083001 -0.0082235671142687761 -
0.20614605213970352" Quaternion="LeftFoot 1 0 0
0"/>
  <GEOM ID="LeftFootPP3Contact" Type="Sphere"
BodyID="LeftFoot" Radius="0.0219"
SpringConstant="2e6" ContactSoftERP="0.1"
Mu="1.0" Abort="false" Position="LeftFoot
0.15507215606083002 0.11787643288573124 -
0.20214605213970352" Quaternion="LeftFoot 1 0 0
0"/>
  <GEOM ID="RightHandPP1Contact" Type="Sphere"
BodyID="RightHand" Radius="0.013"
SpringConstant="2e6" ContactSoftERP="0.1"
Mu="1.0" Abort="false" Position="RightHand
0.057832694976312604 0.048296381316189962 -
0.06972426136581901" Quaternion="RightHand 1 0
0 0"/>
  <GEOM ID="RightHandPP3Contact" Type="Sphere"
BodyID="RightHand" Radius="0.013"
SpringConstant="2e6" ContactSoftERP="0.1"
Mu="1.0" Abort="false" Position="RightHand
0.060732694976312618 -0.033103618683810038 -
0.06972426136581901" Quaternion="RightHand 1 0
0 0"/>
  <GEOM ID="LeftHandPP1Contact" Type="Sphere"
BodyID="LeftHand" Radius="0.013"
SpringConstant="2e6" ContactSoftERP="0.1"
Mu="1.0" Abort="false" Position="LeftHand
0.057832694976307719 -0.048296381316182441 -
0.069724261365819981" Quaternion="LeftHand 1 0
0 0"/>
  <GEOM ID="LeftHandPP3Contact" Type="Sphere"
BodyID="LeftHand" Radius="0.013"
SpringConstant="2e6" ContactSoftERP="0.1"
Mu="1.0" Abort="false" Position="LeftHand
0.060732694976307733 0.033103618683817559 -
0.069724261365819981" Quaternion="LeftHand 1 0
0 0"/>
  <MUSCLE Type="MinettiAlexanderExtended"
Strap="TwoPoint" ID="RightDeepDorsalGroup"
OriginBodyID="HT" InsertionBodyID="RightThigh"
PCA=" 0.151664796 " FibreLength=" 0.104205 "
ForcePerUnitArea="300000" VMaxFactor="8"
ActivationK="0.17" SerialStrainAtFmax="0.06"
ParallelStrainAtFmax="0.6"
ActivationKinetics="false"
TendonLength="0.06232791" Origin="HT -
0.20002914663684154 -0.17979421989852226
0.23615796774176201" Insertion="RightThigh
0.066342129366240732 0.0065714859819235028
0.27768244028130451"/>
  <MUSCLE Type="MinettiAlexanderExtended"
Strap="CylinderWrap"
ID="RightTricepsFemorisGroup" OriginBodyID="HT"
InsertionBodyID="RightShank"
CylinderBodyID="RightShank" PCA=" 0.017856488 "
FibreLength=" 0.663802 "
ForcePerUnitArea="300000" VMaxFactor="8"
ActivationK="0.17" SerialStrainAtFmax="0.06"
ParallelStrainAtFmax="0.6"
ActivationKinetics="false"
TendonLength="0.128012601" Origin="HT -
0.037829146636841574 -0.15109421989852226
0.12665796774176208" Insertion="RightShank
0.14707574374667542 -0.019173708213004903
0.13024051773426182"
CylinderPosition="RightShank
0.10547574374667545 0.034826291786995062
0.2675405177342618"
CylinderRadius="0.10000000000000001"
CylinderQuaternion="RightShank -
0.70710678100000002 0.70710678100000002 0 0"/>
  <MUSCLE Type="MinettiAlexanderExtended"
Strap="CylinderWrap"
ID="RightFemoroTibialisGroup"
OriginBodyID="RightThigh"
InsertionBodyID="RightShank"
CylinderBodyID="RightShank" PCA=" 0.075716382 "
FibreLength=" 0.156547 "
ForcePerUnitArea="300000" VMaxFactor="8"
ActivationK="0.17" SerialStrainAtFmax="0.06"
ParallelStrainAtFmax="0.6"
ActivationKinetics="false"
TendonLength="0.39132054599999999"
Origin="RightThigh 0.075142129366240762
0.021171485981923505 0.037382440281304552"
Insertion="RightShank 0.14707574374667542 -
0.019173708213004903 0.13024051773426182"
CylinderPosition="RightShank
0.10547574374667545 0.034826291786995062
0.2675405177342618"
CylinderRadius="0.10000000000000001"
CylinderQuaternion="RightShank -
0.70710678100000002 0.70710678100000002 0 0"/>
  <MUSCLE Type="MinettiAlexanderExtended"
Strap="TwoPoint" ID="RightCaudoFemoralisGroup"
OriginBodyID="HT" InsertionBodyID="RightThigh"
PCA=" 0.063139805 " FibreLength=" 0.375458 "
ForcePerUnitArea="300000" VMaxFactor="8"
ActivationK="0.17" SerialStrainAtFmax="0.06"
ParallelStrainAtFmax="0.6"
ActivationKinetics="false"
TendonLength="0.53659248699999995" Origin="HT -
1.1549291466368414 -0.083894219898522249
0.29665796774176201" Insertion="RightThigh -
0.0032578706337592633 0.029871485981923518 -
0.0063175597186955201"/>
  <MUSCLE Type="MinettiAlexanderExtended"
Strap="TwoPoint" ID="RightFlexorCrurisGroup"
OriginBodyID="HT" InsertionBodyID="RightShank"
PCA=" 0.030344782 " FibreLength=" 0.520822 "
```

```
ForcePerUnitArea="300000" VMaxFactor="8"
ActivationK="0.17" SerialStrainAtFmax="0.06"
ParallelStrainAtFmax="0.6"
ActivationKinetics="false"
TendonLength="0.41878636000000002" Origin="HT -
0.71612914663684157 -0.098194219898522256
0.29305796774176196" Insertion="RightShank -
0.021624256253324536 0.026026291786995087
0.17714051773426176"/>
  <MUSCLE Type="MinettiAlexanderExtended"
Strap="CylinderWrap"
ID="RightGastrocnemiusLateralis+FD"
OriginBodyID="RightThigh"
InsertionBodyID="RightFoot"
CylinderBodyID="RightFoot" PCA=" 0.055201899 "
FibreLength=" 0.214724 "
ForcePerUnitArea="300000" VMaxFactor="8"
ActivationK="0.17" SerialStrainAtFmax="0.06"
ParallelStrainAtFmax="0.6"
ActivationKinetics="false"
TendonLength="0.68294359500000001"
Origin="RightThigh 0.069942129366240724 -
0.014728514018076511 -0.21981755971869554"
Insertion="RightFoot -0.040527843939169528 -
0.0070764328857305381 0.002753947860296424"
CylinderPosition="RightFoot -
0.051627843939169527 0.015173567114269454
0.10635394786029645"
CylinderRadius="0.059999999999999998"
CylinderQuaternion="RightFoot
0.70710678100000002 0.70710678100000002 0 0"/>
  <MUSCLE Type="MinettiAlexanderExtended"
Strap="CylinderWrap"
ID="RightGastrocnemiusMedialis"
OriginBodyID="RightShank"
InsertionBodyID="RightFoot"
CylinderBodyID="RightFoot" PCA=" 0.251633001 "
FibreLength=" 0.047105 "
ForcePerUnitArea="300000" VMaxFactor="8"
ActivationK="0.17" SerialStrainAtFmax="0.06"
ParallelStrainAtFmax="0.6"
ActivationKinetics="false"
TendonLength="0.62518922899999996"
Origin="RightShank -0.021624256253324536
0.026026291786995087 0.17714051773426176"
Insertion="RightFoot -0.040527843939169528 -
0.0070764328857305381 0.002753947860296424"
CylinderPosition="RightFoot -
0.051627843939169527 0.015173567114269454
0.10635394786029645"
CylinderRadius="0.059999999999999998"
CylinderQuaternion="RightFoot
0.70710678100000002 0.70710678100000002 0 0"/>
  <MUSCLE Type="MinettiAlexanderExtended"
Strap="TwoPoint" ID="RightTibialisAnterior+ED"
OriginBodyID="RightShank"
InsertionBodyID="RightFoot" PCA=" 0.190648998 "
FibreLength=" 0.082897 "
ForcePerUnitArea="300000" VMaxFactor="8"
ActivationK="0.17" SerialStrainAtFmax="0.06"
ParallelStrainAtFmax="0.6"
ActivationKinetics="false"
TendonLength="0.40996096100000001"
Origin="RightShank 0.075675743746675461
0.013626291786995065 0.026640517734261793"
Insertion="RightFoot 0.0045721560608305012 -
0.0022764328857305394 0.002653947860296435"/>
  <MUSCLE Type="MinettiAlexanderExtended"
Strap="TwoPoint" ID="LeftDeepDorsalGroup"
OriginBodyID="HT" InsertionBodyID="LeftThigh"
PCA=" 0.151664796 " FibreLength=" 0.104205 "
ForcePerUnitArea="300000" VMaxFactor="8"
ActivationK="0.17" SerialStrainAtFmax="0.06"
ParallelStrainAtFmax="0.6"
ActivationKinetics="false"
TendonLength="0.06232791" Origin="HT -
0.20002914663684154 0.17960578010147774
0.236157967741762O1" Insertion="LeftThigh
0.066342129366240343 -0.0065714859819230032
0.27768244028130429"/>
  <MUSCLE Type="MinettiAlexanderExtended"
Strap="CylinderWrap"
ID="LeftTricepsFemorisGroup" OriginBodyID="HT"
InsertionBodyID="LeftShank"
CylinderBodyID="LeftShank" PCA=" 0.017856488 "
FibreLength=" 0.663802 "
ForcePerUnitArea="300000" VMaxFactor="8"
ActivationK="0.17" SerialStrainAtFmax="0.06"
ParallelStrainAtFmax="0.6"
ActivationKinetics="false"
TendonLength="0.128012601" Origin="HT -
0.037829146636841574 0.15090578010147773
0.12665796774176208" Insertion="LeftShank
0.14707574374667554 0.019173708213004681
0.13024051773426226"
CylinderPosition="LeftShank 0.10547574374667557
-0.034826291786995284 0.26754051773426224"
CylinderRadius="0.10000000000000001"
CylinderQuaternion="LeftShank -
0.70710678100000002 0.70710678100000002 0 0"/>
  <MUSCLE Type="MinettiAlexanderExtended"
Strap="CylinderWrap"
ID="LeftFemoroTibialisGroup"
OriginBodyID="LeftThigh"
InsertionBodyID="LeftShank"
CylinderBodyID="LeftShank" PCA=" 0.075716382 "
FibreLength=" 0.156547 "
ForcePerUnitArea="300000" VMaxFactor="8"
ActivationK="0.17" SerialStrainAtFmax="0.06"
ParallelStrainAtFmax="0.6"
ActivationKinetics="false"
TendonLength="0.39132054599999999"
Origin="LeftThigh 0.075142129366240373 -
0.021171485981923005 0.037382440281304333"
Insertion="LeftShank 0.14707574374667554
0.019173708213004681 0.13024051773426226"
CylinderPosition="LeftShank 0.10547574374667557
-0.034826291786995284 0.26754051773426224"
CylinderRadius="0.10000000000000001"
CylinderQuaternion="LeftShank -
0.70710678100000002 0.70710678100000002 0 0"/>
  <MUSCLE Type="MinettiAlexanderExtended"
Strap="TwoPoint" ID="LeftCaudoFemoralisGroup"
OriginBodyID="HT" InsertionBodyID="LeftThigh"
PCA=" 0.063139805 " FibreLength=" 0.375458 "
ForcePerUnitArea="300000" VMaxFactor="8"
```

```
ActivationK="0.17" SerialStrainAtFmax="0.06"
ParallelStrainAtFmax="0.6"
ActivationKinetics="false"
TendonLength="0.53659248699999995" Origin="HT -
1.1549291466368414 0.08370578010147775
0.29665796774176201" Insertion="LeftThigh -
0.0032578706337596519 -0.029871485981923018 -
0.0063175597186957422"/>
  <MUSCLE Type="MinettiAlexanderExtended"
Strap="TwoPoint" ID="LeftFlexorCrurisGroup"
OriginBodyID="HT" InsertionBodyID="LeftShank"
PCA=" 0.030344782 " FibreLength=" 0.520822 "
ForcePerUnitArea="300000" VMaxFactor="8"
ActivationK="0.17" SerialStrainAtFmax="0.06"
ParallelStrainAtFmax="0.6"
ActivationKinetics="false"
TendonLength="0.41878636000000002" Origin="HT -
0.71612914663684157 0.098005780101477757
0.29305796774176196" Insertion="LeftShank -
0.021624256253324425 -0.026026291786995309
0.1771405177342622"/>
  <MUSCLE Type="MinettiAlexanderExtended"
Strap="CylinderWrap"
ID="LeftGastrocnemiusLateralis+FD"
OriginBodyID="LeftThigh"
InsertionBodyID="LeftFoot"
CylinderBodyID="LeftFoot" PCA=" 0.055201899 "
FibreLength=" 0.214724 "
ForcePerUnitArea="300000" VMaxFactor="8"
ActivationK="0.17" SerialStrainAtFmax="0.06"
ParallelStrainAtFmax="0.6"
ActivationKinetics="false"
TendonLength="0.68294359500000001"
Origin="LeftThigh 0.069942129366240335
0.01472851401807701 -0.21981755971869577"
Insertion="LeftFoot -0.040527843939169972
0.007076432885731232 0.0027539478602964795"
CylinderPosition="LeftFoot -
0.051627843939169971 -0.01517356711426876
0.1063539478602965"
CylinderRadius="0.059999999999999998"
CylinderQuaternion="LeftFoot
0.70710678100000002 0.70710678100000002 0 0"/>
  <MUSCLE Type="MinettiAlexanderExtended"
Strap="CylinderWrap"
ID="LeftGastrocnemiusMedialis"
OriginBodyID="LeftShank"
InsertionBodyID="LeftFoot"
CylinderBodyID="LeftFoot" PCA=" 0.251633001 "
FibreLength=" 0.047105 "
ForcePerUnitArea="300000" VMaxFactor="8"
ActivationK="0.17" SerialStrainAtFmax="0.06"
ParallelStrainAtFmax="0.6"
ActivationKinetics="false"
TendonLength="0.62518922899999996"
Origin="LeftShank -0.021624256253324425 -
0.026026291786995309 0.1771405177342622"
Insertion="LeftFoot -0.040527843939169972
0.007076432885731232 0.0027539478602964795"
CylinderPosition="LeftFoot -
0.051627843939169971 -0.01517356711426876
0.1063539478602965"
CylinderRadius="0.059999999999999998"
CylinderQuaternion="LeftFoot
0.70710678100000002 0.70710678100000002 0 0"/>
  <MUSCLE Type="MinettiAlexanderExtended"
Strap="TwoPoint" ID="LeftTibialisAnterior+ED"
OriginBodyID="LeftShank"
InsertionBodyID="LeftFoot" PCA=" 0.190648998 "
FibreLength=" 0.082897 "
ForcePerUnitArea="300000" VMaxFactor="8"
ActivationK="0.17" SerialStrainAtFmax="0.06"
ParallelStrainAtFmax="0.6"
ActivationKinetics="false"
TendonLength="0.40996096100000001"
Origin="LeftShank 0.075675743746675572 -
0.013626291786995287 0.026640517734262237"
Insertion="LeftFoot 0.0045721560608300571
0.0022764328857312333 0.0026539478602964905"/>
  <MUSCLE Type="MinettiAlexanderExtended"
Strap="TwoPoint" ID="RightShoulderFlexors"
OriginBodyID="HT" InsertionBodyID="RightArm"
PCA=" 0.027493045 " FibreLength=" 0.246362 "
ForcePerUnitArea="300000" VMaxFactor="8"
ActivationK="0.17" SerialStrainAtFmax="0.06"
ParallelStrainAtFmax="0.6"
ActivationKinetics="false"
TendonLength="0.29325024999999999" Origin="HT
0.56887085336315846 -0.24859421989852226 -
0.30144203225823785" Insertion="RightArm
0.029188632066430298 -0.021156755599971794
0.023391466416864848"/>
  <MUSCLE Type="MinettiAlexanderExtended"
Strap="CylinderWrap"
ID="RightShoulderExtensors" OriginBodyID="HT"
InsertionBodyID="RightArm"
CylinderBodyID="RightArm" PCA=" 0.161703997 "
FibreLength=" 0.06283 "
ForcePerUnitArea="300000" VMaxFactor="8"
ActivationK="0.17" SerialStrainAtFmax="0.06"
ParallelStrainAtFmax="0.6"
ActivationKinetics="false"
TendonLength="0.485243588" Origin="HT
0.82517085336315843 -0.18599421989852227 -
0.322242032258238" Insertion="RightArm
0.069988632066430356 -0.016256755599971806 -
0.014208533583135119"
CylinderPosition="RightArm 0.13183863206643032
0.015643244400028206 0.19924146641686491"
CylinderRadius="0.040000000000000001"
CylinderQuaternion="RightArm -
0.70710678100000002 0.70710678100000002 0 0"/>
  <MUSCLE Type="MinettiAlexanderExtended"
Strap="CylinderWrap" ID="RightTricepsBrachii"
OriginBodyID="HT"
InsertionBodyID="RightForearm"
CylinderBodyID="RightForearm" PCA=" 0.029642022
" FibreLength=" 0.171376 "
ForcePerUnitArea="300000" VMaxFactor="8"
ActivationK="0.17" SerialStrainAtFmax="0.06"
ParallelStrainAtFmax="0.6"
ActivationKinetics="false"
TendonLength="0.23191341900000001" Origin="HT
0.80817085336315841 -0.17609421989852225 -
0.58584203225823794" Insertion="RightForearm -
0.10957816135674514 -0.019710035981314711
```

```
0.14202774699567011"
CylinderPosition="RightForearm -
0.084878161356745085 0.0024899640186852867
0.17122774699567006"
CylinderRadius="0.029999999999999999"
CylinderQuaternion="RightForearm
0.70710678100000002 0.70710678100000002 0 0"/>
  <MUSCLE Type="MinettiAlexanderExtended"
Strap="CylinderWrap" ID="RightBicepsBrachii"
OriginBodyID="HT"
InsertionBodyID="RightForearm"
CylinderBodyID="RightArm" PCA=" 0.021103596 "
FibreLength=" 0.160476 "
ForcePerUnitArea="300000" VMaxFactor="8"
ActivationK="0.17" SerialStrainAtFmax="0.06"
ParallelStrainAtFmax="0.6"
ActivationKinetics="false"
TendonLength="0.30081610399999997" Origin="HT
0.93067085336315836 -0.15539421989852226 -
0.55494203225823791" Insertion="RightForearm -
0.025978161356745133 -0.01811003598131472
0.13442774699567012" CylinderPosition="RightArm
0.13183863206643032 0.015643244400028206
0.19924146641686491"
CylinderRadius="0.040000000000000001"
CylinderQuaternion="RightArm -
0.70710678100000002 0.70710678100000002 0 0"/>
  <MUSCLE Type="MinettiAlexanderExtended"
Strap="TwoPoint" ID="RightElbowFlexors"
OriginBodyID="RightArm"
InsertionBodyID="RightForearm" PCA="
0.034570053 " FibreLength=" 0.097964 "
ForcePerUnitArea="300000" VMaxFactor="8"
ActivationK="0.17" SerialStrainAtFmax="0.06"
ParallelStrainAtFmax="0.6"
ActivationKinetics="false"
TendonLength="0.016623651999999999"
Origin="RightArm 0.001288632066430373 -
0.0093567555999717889 -0.034008533583135159"
Insertion="RightForearm -0.025978161356745133 -
0.01811003598131472 0.13442774699567012"/>
  <MUSCLE Type="MinettiAlexanderExtended"
Strap="CylinderWrap" ID="RightElbowExtensors"
OriginBodyID="RightArm"
InsertionBodyID="RightForearm"
CylinderBodyID="RightForearm" PCA=" 0.107989436
" FibreLength=" 0.047041 "
ForcePerUnitArea="300000" VMaxFactor="8"
ActivationK="0.17" SerialStrainAtFmax="0.06"
ParallelStrainAtFmax="0.6"
ActivationKinetics="false"
TendonLength="0.138083762" Origin="RightArm -
0.033811367933569647 -0.0056567555999718078
0.013691466416864917" Insertion="RightForearm -
0.10957816135674514 -0.019710035981314711
0.14202774699567011"
CylinderPosition="RightForearm -
0.084878161356745085 0.0024899640186852867
0.17122774699567006"
CylinderRadius="0.029999999999999999"
CylinderQuaternion="RightForearm
0.70710678100000002 0.70710678100000002 0 0"/>
  <MUSCLE Type="MinettiAlexanderExtended"
Strap="CylinderWrap" ID="RightWristFlexors"
OriginBodyID="RightForearm"
InsertionBodyID="RightHand"
CylinderBodyID="RightHand" PCA=" 0.252337435 "
FibreLength=" 0.026842 "
ForcePerUnitArea="300000" VMaxFactor="8"
ActivationK="0.17" SerialStrainAtFmax="0.06"
ParallelStrainAtFmax="0.6"
ActivationKinetics="false"
TendonLength="0.31183402999999998"
Origin="RightForearm -0.092578161356745126 -
0.017010035981314703 0.080127746995670102"
Insertion="RightHand -0.045567305023687443 -
0.0092036186838100331 0.079975738634181004"
CylinderPosition="RightHand -
0.071417305023687372 -0.0068036186838100476
0.13302573863418099"
CylinderRadius="0.029999999999999999"
CylinderQuaternion="RightHand
0.70710678100000002 0.70710678100000002 0 0"/>
  <MUSCLE Type="MinettiAlexanderExtended"
Strap="CylinderWrap" ID="RightWristExtensors"
OriginBodyID="RightForearm"
InsertionBodyID="RightHand"
CylinderBodyID="RightHand" PCA=" 0.323480074 "
FibreLength=" 0.031408 "
ForcePerUnitArea="300000" VMaxFactor="8"
ActivationK="0.17" SerialStrainAtFmax="0.06"
ParallelStrainAtFmax="0.6"
ActivationKinetics="false"
TendonLength="0.336866043" Origin="RightForearm
-0.054378161356745114 0.027589964018685298
0.12252774699567009" Insertion="RightHand -
0.017067305023687362 -0.005603618683810041
0.079375738634180987"
CylinderPosition="RightHand -
0.071417305023687372 -0.0068036186838100476
0.13302573863418099"
CylinderRadius="0.040000000000000001"
CylinderQuaternion="RightHand -
0.70710678100000002 0.70710678100000002 0 0"/>
  <MUSCLE Type="MinettiAlexanderExtended"
Strap="TwoPoint" ID="LeftShoulderFlexors"
OriginBodyID="HT" InsertionBodyID="LeftArm"
PCA=" 0.027493045 " FibreLength=" 0.246362 "
ForcePerUnitArea="300000" VMaxFactor="8"
ActivationK="0.17" SerialStrainAtFmax="0.06"
ParallelStrainAtFmax="0.6"
ActivationKinetics="false"
TendonLength="0.29325024999999999" Origin="HT
0.56887085336315846 0.24840578010147774 -
0.30144203225823785" Insertion="LeftArm
0.029188632066430742 0.021156755599971627
0.023391466416865625"/>
  <MUSCLE Type="MinettiAlexanderExtended"
Strap="CylinderWrap" ID="LeftShoulderExtensors"
OriginBodyID="HT" InsertionBodyID="LeftArm"
CylinderBodyID="LeftArm" PCA=" 0.161703997 "
FibreLength=" 0.06283 "
ForcePerUnitArea="300000" VMaxFactor="8"
ActivationK="0.17" SerialStrainAtFmax="0.06"
ParallelStrainAtFmax="0.6"
```

```
ActivationKinetics="false"
TendonLength="0.485243588" Origin="HT
0.82517085336315843 0.18580578010147775 -
0.322242032258238" Insertion="LeftArm
0.0699886320664308 0.01625675559997164 -
0.014208533583134342" CylinderPosition="LeftArm
0.13183863206643076 -0.015643244400028372
0.19924146641686569"
CylinderRadius="0.040000000000000001"
CylinderQuaternion="LeftArm -
0.70710678100000002 0.70710678100000002 0 0"/>
  <MUSCLE Type="MinettiAlexanderExtended"
Strap="CylinderWrap" ID="LeftTricepsBrachii"
OriginBodyID="HT" InsertionBodyID="LeftForearm"
CylinderBodyID="LeftForearm" PCA=" 0.029642022
" FibreLength=" 0.171376 "
ForcePerUnitArea="300000" VMaxFactor="8"
ActivationK="0.17" SerialStrainAtFmax="0.06"
ParallelStrainAtFmax="0.6"
ActivationKinetics="false"
TendonLength="0.23191341900000001" Origin="HT
0.80817085336315841 0.17590578010147773 -
0.58584203225823794" Insertion="LeftForearm -
0.10957816135674003 0.019710035981316404
0.14202774699567322"
CylinderPosition="LeftForearm -
0.084878161356739978 -0.0024899640186835936
0.17122774699567317"
CylinderRadius="0.029999999999999999"
CylinderQuaternion="LeftForearm
0.70710678100000002 0.70710678100000002 0 0"/>
  <MUSCLE Type="MinettiAlexanderExtended"
Strap="CylinderWrap" ID="LeftBicepsBrachii"
OriginBodyID="HT" InsertionBodyID="LeftForearm"
CylinderBodyID="LeftArm" PCA=" 0.021103596 "
FibreLength=" 0.160476 "
ForcePerUnitArea="300000" VMaxFactor="8"
ActivationK="0.17" SerialStrainAtFmax="0.06"
ParallelStrainAtFmax="0.6"
ActivationKinetics="false"
TendonLength="0.30081610399999997" Origin="HT
0.93067085336315836 0.15520578010147773 -
0.55494203225823791" Insertion="LeftForearm -
0.025978161356740026 0.018110035981316414
0.13442774699567323" CylinderPosition="LeftArm
0.13183863206643076 -0.015643244400028372
0.19924146641686569"
CylinderRadius="0.040000000000000001"
CylinderQuaternion="LeftArm -
0.70710678100000002 0.70710678100000002 0 0"/>
  <MUSCLE Type="MinettiAlexanderExtended"
Strap="TwoPoint" ID="LeftElbowFlexors"
OriginBodyID="LeftArm"
InsertionBodyID="LeftForearm" PCA=" 0.034570053
" FibreLength=" 0.097964 "
ForcePerUnitArea="300000" VMaxFactor="8"
ActivationK="0.17" SerialStrainAtFmax="0.06"
ParallelStrainAtFmax="0.6"
ActivationKinetics="false"
TendonLength="0.016623651999999999"
Origin="LeftArm 0.0012886320664308171
0.0093567555999716223 -0.034008533583134382"
Insertion="LeftForearm -0.025978161356740026
0.018110035981316414 0.13442774699567323"/>
  <MUSCLE Type="MinettiAlexanderExtended"
Strap="CylinderWrap" ID="LeftElbowExtensors"
OriginBodyID="LeftArm"
InsertionBodyID="LeftForearm"
CylinderBodyID="LeftForearm" PCA=" 0.107989436
" FibreLength=" 0.047041 "
ForcePerUnitArea="300000" VMaxFactor="8"
ActivationK="0.17" SerialStrainAtFmax="0.06"
ParallelStrainAtFmax="0.6"
ActivationKinetics="false"
TendonLength="0.138083762" Origin="LeftArm -
0.033811367933569203 0.0056567555999716412
0.013691466416865694" Insertion="LeftForearm -
0.10957816135674003 0.019710035981316404
0.14202774699567322"
CylinderPosition="LeftForearm -
0.084878161356739978 -0.0024899640186835936
0.17122774699567317"
CylinderRadius="0.029999999999999999"
CylinderQuaternion="LeftForearm
0.70710678100000002 0.70710678100000002 0 0"/>
  <MUSCLE Type="MinettiAlexanderExtended"
Strap="CylinderWrap" ID="LeftWristFlexors"
OriginBodyID="LeftForearm"
InsertionBodyID="LeftHand"
CylinderBodyID="LeftHand" PCA=" 0.252337435 "
FibreLength=" 0.026842 "
ForcePerUnitArea="300000" VMaxFactor="8"
ActivationK="0.17" SerialStrainAtFmax="0.06"
ParallelStrainAtFmax="0.6"
ActivationKinetics="false"
TendonLength="0.31183402999999998"
Origin="LeftForearm -0.092578161356740019
0.017010035981316396 0.08012774699567321"
Insertion="LeftHand -0.045567305023692328
0.0092036186838175549 0.079975738634180032"
CylinderPosition="LeftHand -
0.071417305023692257 0.0068036186838175694
0.13302573863418002"
CylinderRadius="0.029999999999999999"
CylinderQuaternion="LeftHand
0.70710678100000002 0.70710678100000002 0 0"/>
  <MUSCLE Type="MinettiAlexanderExtended"
Strap="CylinderWrap" ID="LeftWristExtensors"
OriginBodyID="LeftForearm"
InsertionBodyID="LeftHand"
CylinderBodyID="LeftHand" PCA=" 0.323480074 "
FibreLength=" 0.031408 "
ForcePerUnitArea="300000" VMaxFactor="8"
ActivationK="0.17" SerialStrainAtFmax="0.06"
ParallelStrainAtFmax="0.6"
ActivationKinetics="false"
TendonLength="0.336866043" Origin="LeftForearm
-0.054378161356740007 -0.027589964018683605
0.1225277469956732" Insertion="LeftHand -
0.017067305023692247 0.0056036186838175628
0.079375738634180015"
CylinderPosition="LeftHand -
0.071417305023692257 0.0068036186838175694
0.13302573863418002"
CylinderRadius="0.040000000000000001"
```

```
CylinderQuaternion="LeftHand -
0.70710678100000002 0.70710678100000002 0 0"/>
  <DRIVER Type="Cyclic"
ID="LeftBicepsBrachiiDriver"
Target="LeftBicepsBrachii"
DurationValuePairs="0.05910085049468791
1.0000000000000000 0.05910085049468791
0.62935368596926422 0.05910085049468791
0.0000000000000000 0.05910085049468791
0.80575858341942563 0.05910085049468791
0.58969497212428901 0.05910085049468791
0.0000000000000000 0.05910085049468791
0.0000000000000000 0.05910085049468791
0.08932690255880904 0.05910085049468791
0.46342069114290785 0.05910085049468791
0.81660545118895234"/>
  <DRIVER Type="Cyclic"
ID="LeftCaudoFemoralisGroupDriver"
Target="LeftCaudoFemoralisGroup"
DurationValuePairs="0.05910085049468791
0.0000000000000000 0.05910085049468791
0.98593775876718692 0.05910085049468791
0.99018127067199369 0.05910085049468791
0.51249751751913042 0.05910085049468791
0.0000000000000000 0.05910085049468791
0.56178881043795803 0.05910085049468791
1.0000000000000000 0.05910085049468791
1.0000000000000000 0.05910085049468791
0.83701294962250028 0.05910085049468791
0.0000000000000000"/>
  <DRIVER Type="Cyclic"
ID="LeftFemoroTibialisGroupDriver"
Target="LeftFemoroTibialisGroup"
DurationValuePairs="0.05910085049468791
0.15425197654417144 0.05910085049468791
0.05666610370429177 0.05910085049468791
0.0000000000000000 0.05910085049468791
0.0000000000000000 0.05910085049468791
0.34183543104734543 0.05910085049468791
1.0000000000000000 0.05910085049468791
0.0000000000000000 0.05910085049468791
0.93078678632199419 0.05910085049468791
0.72856309698750576 0.05910085049468791
0.01514252711560308"/>
  <DRIVER Type="Cyclic"
ID="LeftDeepDorsalGroupDriver"
Target="LeftDeepDorsalGroup"
DurationValuePairs="0.05910085049468791
1.0000000000000000 0.05910085049468791
1.0000000000000000 0.05910085049468791
0.0000000000000000 0.05910085049468791
1.0000000000000000 0.05910085049468791
0.97017786804174067 0.05910085049468791
1.0000000000000000 0.05910085049468791
0.0000000000000000 0.05910085049468791
0.0000000000000000 0.05910085049468791
0.02327125118170864 0.05910085049468791
0.97168507585576036"/>
  <DRIVER Type="Cyclic"
ID="LeftElbowExtensorsDriver"
Target="LeftElbowExtensors"
DurationValuePairs="0.05910085049468791
0.22018120444986117 0.05910085049468791
1.0000000000000000 0.05910085049468791
0.45823252366289385 0.05910085049468791
0.40497842930603778 0.05910085049468791
0.57080484569195100 0.05910085049468791
1.0000000000000000 0.05910085049468791
1.0000000000000000 0.05910085049468791
0.24144261036288531 0.05910085049468791
0.86503133931946474 0.05910085049468791
0.0000000000000000"/>
  <DRIVER Type="Cyclic"
ID="LeftElbowFlexorsDriver"
Target="LeftElbowFlexors"
DurationValuePairs="0.05910085049468791
0.80104774762759023 0.05910085049468791
0.08397004476415967 0.05910085049468791
0.0000000000000000 0.05910085049468791
0.13828662242324471 0.05910085049468791
0.86184762721238395 0.05910085049468791
0.01318006553841108 0.05910085049468791
0.00512758186811628 0.05910085049468791
0.83709138967329477 0.05910085049468791
0.61916125379832332 0.05910085049468791
0.73024779257377370"/>
  <DRIVER Type="Cyclic"
ID="LeftFlexorCrurisGroupDriver"
Target="LeftFlexorCrurisGroup"
DurationValuePairs="0.05910085049468791
0.0000000000000000 0.05910085049468791
0.22227108158918849 0.05910085049468791
0.98962881915555534 0.05910085049468791
0.46560708542331414 0.05910085049468791
0.00319998549364489 0.05910085049468791
0.0000000000000000 0.05910085049468791
1.0000000000000000 0.05910085049468791
1.0000000000000000 0.05910085049468791
0.56812999635947803 0.05910085049468791
0.0000000000000000"/>
  <DRIVER Type="Cyclic"
ID="LeftGastrocnemiusLateralis+FDDriver"
Target="LeftGastrocnemiusLateralis+FD"
DurationValuePairs="0.05910085049468791
0.80486833093895160 0.05910085049468791
0.46571344795623010 0.05910085049468791
0.80728859922299034 0.05910085049468791
0.51393748064067690 0.05910085049468791
0.0000000000000000 0.05910085049468791
0.68238327006427613 0.05910085049468791
1.0000000000000000 0.05910085049468791
1.0000000000000000 0.05910085049468791
0.78267854142169724 0.05910085049468791
1.0000000000000000"/>
  <DRIVER Type="Cyclic"
ID="LeftGastrocnemiusMedialisDriver"
Target="LeftGastrocnemiusMedialis"
DurationValuePairs="0.05910085049468791
0.97213955839825328 0.05910085049468791
0.98905808089800884 0.05910085049468791
0.91045349631499961 0.05910085049468791
1.0000000000000000 0.05910085049468791
0.0000000000000000 0.05910085049468791
0.91398792212170621 0.05910085049468791
0.97864554868246334 0.05910085049468791
0.82717167275121806 0.05910085049468791
```

```
0.98968302000233233 0.05910085049468791
0.00000000000000000"/>
  <DRIVER Type="Cyclic"
ID="LeftShoulderExtensorsDriver"
Target="LeftShoulderExtensors"
DurationValuePairs="0.05910085049468791
0.67858654199710011 0.05910085049468791
0.60021005491441060 0.05910085049468791
0.00000000000000000 0.05910085049468791
0.78963369437501318 0.05910085049468791
0.84242401848962145 0.05910085049468791
0.49063258719791741 0.05910085049468791
0.00529713152169739 0.05910085049468791
0.66875606415876887 0.05910085049468791
0.88997057138794000 0.05910085049468791
0.02504267079345886"/>
  <DRIVER Type="Cyclic"
ID="LeftShoulderFlexorsDriver"
Target="LeftShoulderFlexors"
DurationValuePairs="0.05910085049468791
0.04676334318056265 0.05910085049468791
0.00000000000000000 0.05910085049468791
0.82449598722605977 0.05910085049468791
0.88645385565839196 0.05910085049468791
0.00000000000000000 0.05910085049468791
0.01054320590736503 0.05910085049468791
1.00000000000000000 0.05910085049468791
0.68959891641945859 0.05910085049468791
0.59002459736830792 0.05910085049468791
0.53693039994264069"/>
  <DRIVER Type="Cyclic"
ID="LeftTibialisAnterior+EDDriver"
Target="LeftTibialisAnterior+ED"
DurationValuePairs="0.05910085049468791
1.00000000000000000 0.05910085049468791
1.00000000000000000 0.05910085049468791
0.94884581310418903 0.05910085049468791
0.00000000000000000 0.05910085049468791
0.96233842101299405 0.05910085049468791
0.88579453213524428 0.05910085049468791
0.96057602993312086 0.05910085049468791
0.92362040296694581 0.05910085049468791
0.00000000000000000 0.05910085049468791
0.98695363412806758"/>
  <DRIVER Type="Cyclic"
ID="LeftTricepsBrachiiDriver"
Target="LeftTricepsBrachii"
DurationValuePairs="0.05910085049468791
0.09354252305338490 0.05910085049468791
0.00000000000000000 0.05910085049468791
0.76725810340742617 0.05910085049468791
1.00000000000000000 0.05910085049468791
0.00000000000000000 0.05910085049468791
0.13923808407388202 0.05910085049468791
0.25935252046800916 0.05910085049468791
0.36838665314626495 0.05910085049468791
0.88145705454492296 0.05910085049468791
0.33371815474151600"/>
  <DRIVER Type="Cyclic"
ID="LeftTricepsFemorisGroupDriver"
Target="LeftTricepsFemorisGroup"
DurationValuePairs="0.05910085049468791
0.95429211267256742 0.05910085049468791
1.00000000000000000 0.05910085049468791
0.00577788921026121 0.05910085049468791
0.00000000000000000 0.05910085049468791
0.89999872816875592 0.05910085049468791
0.95931849663083724 0.05910085049468791
0.00000000000000000 0.05910085049468791
0.00000000000000000 0.05910085049468791
0.00000000000000000 0.05910085049468791
0.70034827071699712"/>
  <DRIVER Type="Cyclic"
ID="LeftWristExtensorsDriver"
Target="LeftWristExtensors"
DurationValuePairs="0.05910085049468791
0.06008400321610884 0.05910085049468791
0.09925799322519024 0.05910085049468791
0.52949685282741799 0.05910085049468791
0.25435389783811280 0.05910085049468791
0.04478484459205914 0.05910085049468791
0.91227762604428653 0.05910085049468791
0.00057212098058071 0.05910085049468791
0.86909016488333690 0.05910085049468791
0.78390499764321375 0.05910085049468791
0.15914305004933327"/>
  <DRIVER Type="Cyclic"
ID="LeftWristFlexorsDriver"
Target="LeftWristFlexors"
DurationValuePairs="0.05910085049468791
0.71543848251505615 0.05910085049468791
0.91231756917923124 0.05910085049468791
0.89176171840338125 0.05910085049468791
0.69280353571719355 0.05910085049468791
1.00000000000000000 0.05910085049468791
0.14743692533461678 0.05910085049468791
0.74429685730679573 0.05910085049468791
0.87032443394831027 0.05910085049468791
0.46003004910968109 0.05910085049468791
0.78487982099904308"/>
  <DRIVER Type="Cyclic"
ID="RightBicepsBrachiiDriver"
Target="RightBicepsBrachii"
DurationValuePairs="0.05910085049468791
0.00000000000000000 0.05910085049468791
0.00000000000000000 0.05910085049468791
0.08932690255880904 0.05910085049468791
0.46342069114290785 0.05910085049468791
0.81660545118895234 0.05910085049468791
1.00000000000000000 0.05910085049468791
0.62935368596926422 0.05910085049468791
0.00000000000000000 0.05910085049468791
0.80575858341942563 0.05910085049468791
0.58969497212428901"/>
  <DRIVER Type="Cyclic"
ID="RightCaudoFemoralisGroupDriver"
Target="RightCaudoFemoralisGroup"
DurationValuePairs="0.05910085049468791
0.56178881043795803 0.05910085049468791
1.00000000000000000 0.05910085049468791
1.00000000000000000 0.05910085049468791
0.83701294962250028 0.05910085049468791
0.00000000000000000 0.05910085049468791
0.00000000000000000 0.05910085049468791
0.98593775876718692 0.05910085049468791
0.99018127067199369 0.05910085049468791
```

```
0.51249751751913042 0.05910085049468791
0.00000000000000000"/>
  <DRIVER Type="Cyclic"
ID="RightFemoroTibialisGroupDriver"
Target="RightFemoroTibialisGroup"
DurationValuePairs="0.05910085049468791
1.00000000000000000 0.05910085049468791
0.00000000000000000 0.05910085049468791
0.93078678632199419 0.05910085049468791
0.72856309698750576 0.05910085049468791
0.01514252711560308 0.05910085049468791
0.15425197654417144 0.05910085049468791
0.05666610370429177 0.05910085049468791
0.00000000000000000 0.05910085049468791
0.00000000000000000 0.05910085049468791
0.34183543104734543"/>
  <DRIVER Type="Cyclic"
ID="RightDeepDorsalGroupDriver"
Target="RightDeepDorsalGroup"
DurationValuePairs="0.05910085049468791
1.00000000000000000 0.05910085049468791
0.00000000000000000 0.05910085049468791
0.00000000000000000 0.05910085049468791
0.02327125118170864 0.05910085049468791
0.97168507585576036 0.05910085049468791
1.00000000000000000 0.05910085049468791
1.00000000000000000 0.05910085049468791
0.00000000000000000 0.05910085049468791
1.00000000000000000 0.05910085049468791
0.97017786804174067"/>
  <DRIVER Type="Cyclic"
ID="RightElbowExtensorsDriver"
Target="RightElbowExtensors"
DurationValuePairs="0.05910085049468791
1.00000000000000000 0.05910085049468791
1.00000000000000000 0.05910085049468791
0.24144261036288531 0.05910085049468791
0.86503133931946474 0.05910085049468791
0.00000000000000000 0.05910085049468791
0.22018120444986117 0.05910085049468791
1.00000000000000000 0.05910085049468791
0.45823252366289385 0.05910085049468791
0.40497842930603778 0.05910085049468791
0.57080484569195100"/>
  <DRIVER Type="Cyclic"
ID="RightElbowFlexorsDriver"
Target="RightElbowFlexors"
DurationValuePairs="0.05910085049468791
0.01318006553841108 0.05910085049468791
0.00512758186811628 0.05910085049468791
0.83709138967329477 0.05910085049468791
0.61916125379832332 0.05910085049468791
0.73024779257377370 0.05910085049468791
0.80104774762759023 0.05910085049468791
0.08397004476415967 0.05910085049468791
0.00000000000000000 0.05910085049468791
0.13828662242324471 0.05910085049468791
0.86184762721238395"/>
  <DRIVER Type="Cyclic"
ID="RightFlexorCrurisGroupDriver"
Target="RightFlexorCrurisGroup"
DurationValuePairs="0.05910085049468791
0.00000000000000000 0.05910085049468791
1.00000000000000000 0.05910085049468791
1.00000000000000000 0.05910085049468791
0.56812999635947803 0.05910085049468791
0.00000000000000000 0.05910085049468791
0.00000000000000000 0.05910085049468791
0.22227108158918849 0.05910085049468791
0.98962881915555534 0.05910085049468791
0.46560708542331414 0.05910085049468791
0.00319998549364489"/>
  <DRIVER Type="Cyclic"
ID="RightGastrocnemiusLateralis+FDDriver"
Target="RightGastrocnemiusLateralis+FD"
DurationValuePairs="0.05910085049468791
0.68238327006427613 0.05910085049468791
1.00000000000000000 0.05910085049468791
1.00000000000000000 0.05910085049468791
0.78267854142169724 0.05910085049468791
1.00000000000000000 0.05910085049468791
0.80486833093895160 0.05910085049468791
0.46571344795623010 0.05910085049468791
0.80728859922299034 0.05910085049468791
0.51393748064067690 0.05910085049468791
0.00000000000000000"/>
  <DRIVER Type="Cyclic"
ID="RightGastrocnemiusMedialisDriver"
Target="RightGastrocnemiusMedialis"
DurationValuePairs="0.05910085049468791
0.91398792212170621 0.05910085049468791
0.97864554868246334 0.05910085049468791
0.82717167275121806 0.05910085049468791
0.98968302000233233 0.05910085049468791
0.00000000000000000 0.05910085049468791
0.97213955839825328 0.05910085049468791
0.98905808089800884 0.05910085049468791
0.91045349631499961 0.05910085049468791
1.00000000000000000 0.05910085049468791
0.00000000000000000"/>
  <DRIVER Type="Cyclic"
ID="RightShoulderExtensorsDriver"
Target="RightShoulderExtensors"
DurationValuePairs="0.05910085049468791
0.49063258719791741 0.05910085049468791
0.00529713152169739 0.05910085049468791
0.66875606415876887 0.05910085049468791
0.88997057138794000 0.05910085049468791
0.02504267079345886 0.05910085049468791
0.67858654199710011 0.05910085049468791
0.60021005491441060 0.05910085049468791
0.00000000000000000 0.05910085049468791
0.78963369437501318 0.05910085049468791
0.84242401848962145"/>
  <DRIVER Type="Cyclic"
ID="RightShoulderFlexorsDriver"
Target="RightShoulderFlexors"
DurationValuePairs="0.05910085049468791
0.01054320590736503 0.05910085049468791
1.00000000000000000 0.05910085049468791
0.68959891641945859 0.05910085049468791
0.59002459736830792 0.05910085049468791
0.53693039994264069 0.05910085049468791
0.04676334318056265 0.05910085049468791
0.00000000000000000 0.05910085049468791
0.82449598722605977 0.05910085049468791
```

```
0.88645385565839196 0.05910085049468791
0.00000000000000000"/>
  <DRIVER Type="Cyclic"
ID="RightTibialisAnterior+EDDriver"
Target="RightTibialisAnterior+ED"
DurationValuePairs="0.05910085049468791
0.88579453213524428 0.05910085049468791
0.96057602993312086 0.05910085049468791
0.92362040296694581 0.05910085049468791
0.00000000000000000 0.05910085049468791
0.98695363412806758 0.05910085049468791
1.00000000000000000 0.05910085049468791
1.00000000000000000 0.05910085049468791
0.94884581310418903 0.05910085049468791
0.00000000000000000 0.05910085049468791
0.96233842101299405"/>
  <DRIVER Type="Cyclic"
ID="RightTricepsBrachiiDriver"
Target="RightTricepsBrachii"
DurationValuePairs="0.05910085049468791
0.13923808407388202 0.05910085049468791
0.25935252046800916 0.05910085049468791
0.36838665314626495 0.05910085049468791
0.88145705454492296 0.05910085049468791
0.33371815474151600 0.05910085049468791
0.09354252305338490 0.05910085049468791
0.00000000000000000 0.05910085049468791
0.76725810340742617 0.05910085049468791
1.00000000000000000 0.05910085049468791
0.00000000000000000"/>
  <DRIVER Type="Cyclic"
ID="RightTricepsFemorisGroupDriver"
Target="RightTricepsFemorisGroup"
DurationValuePairs="0.05910085049468791
0.95931849663083724 0.05910085049468791
0.00000000000000000 0.05910085049468791
0.00000000000000000 0.05910085049468791
0.00000000000000000 0.05910085049468791
0.70034827071699712 0.05910085049468791
0.95429211267256742 0.05910085049468791
1.00000000000000000 0.05910085049468791
0.00577788921026121 0.05910085049468791
0.00000000000000000 0.05910085049468791
0.89999872816875592"/>
  <DRIVER Type="Cyclic"
ID="RightWristExtensorsDriver"
Target="RightWristExtensors"
DurationValuePairs="0.05910085049468791
0.91227762604428653 0.05910085049468791
0.00057212098058071 0.05910085049468791
0.86909016488333690 0.05910085049468791
0.78390499764321375 0.05910085049468791
0.15914305004933327 0.05910085049468791
0.06008400321610884 0.05910085049468791
0.09925799322519024 0.05910085049468791
0.52949685282741799 0.05910085049468791
0.25435389783811280 0.05910085049468791
0.04478484459205914"/>
  <DRIVER Type="Cyclic"
ID="RightWristFlexorsDriver"
Target="RightWristFlexors"
DurationValuePairs="0.05910085049468791
0.14743692533461678 0.05910085049468791
0.74429685730679573 0.05910085049468791
0.87032443394831027 0.05910085049468791
0.46003004910968109 0.05910085049468791
0.78487982099904308 0.05910085049468791
0.71543848251505615 0.05910085049468791
0.91231756917923124 0.05910085049468791
0.89176171840338125 0.05910085049468791
0.69280353571719355 0.05910085049468791
1.00000000000000000"/>
</GAITSYMODE>
```